1 **Supporting information**

2

3 *In-situ* **zinc cyanamide coordination induced highly N-rich graphene**

4 **for efficient peroxymonosulfate activation**

5

6 Junjie Zhang [a], Hanwen Liu [a], Wenran Gao [b], Dongfang Cheng [c], Fatang Tan [a], Wei Wang [a, *],

7 Xinyun Wang [a], Xueliang Qiao [a], Po Keung Wong [d], Yonggang Yao [a, *]

8

9 [a] State Key Laboratory of Materials Processing and Die & Mould Technology, School of

10 Materials Science and Engineering, Huazhong University of Science and Technology, Wuhan

11 430074, Hubei, China

12 [b] Joint International Research Laboratory of Biomass Energy and Materials, Co-Innovation

13 Center of Efficient Processing and Utilization of Forest Resources, College of Materials

14 Science and Engineering, Nanjing Forestry University, Nanjing 210037, China

15 [c] Department of Chemical and Biomolecular Engineering, University of California, Los

16 Angeles, Los Angeles, California 90095, United States

17 [d] School of Life Sciences, The Chinese University of Hong Kong, Shatin, NT, Hong Kong

18 SAR, China

19

20 * Corresponding author. E-mail: weiwang@hust.edu.cn; yaoyg@hust.edu.cn

21

22

## S1 Experimental Section

Materials and chemicals: Zinc (Zn) powder, melamine, dicyandiamide, thiourea, hydrochloric acid (HCl), *p*-benzoquinone and ethanol were supplied by Sinopharm Chemical Reagent Co., Ltd.. Tetracycline, cyanamide, furfuryl alcohol, potassium peroxymonosulfate (PMS, 98 wt%), 5,5-dimethyl-pyridine N-oxide (DMPO, 97 wt%) and 2,2,6,6-tetramethylpiperidine (TEMP, 99 wt%) were purchased from Aladdin (China) Reagent Co., Ltd. All chemicals were of analytical grade and used as received without any purification in all experiments.

Preparation of porous ultrahigh nitrogen-doped graphene (NRG) samples: NRG samples were synthesized via the pyrolysis of different N-rich organics (melamine, dicyandiamide or thiourea) at the assistance of zinc catalyst. In a typical procedure, 4 g melamine and 2 g Zn were completely mixed by grinding in an agate mortar. The obtained mixture was added into a combustion boat and annealed at 900 °C in argon (Ar) atmosphere for 2 h with a ramp rate of 10 °C/min. To remove the catalyst, the pyrolysis product was leached overnight using an aqueous solution of 1 M HCl, washed with Milli-Q water several times, and then dried at 60 °C in a vacuum oven. The catalysts prepared with melamine, dicyandiamide and thiourea were donated as NRG-ME, NRG-DI and NRG-TH, respectively. Taking ME as a representative N-rich organics, the effects of pyrolysis temperature (700, 800, 900 and 1000 °C), mass ratio of melamine to Zn (1:1, 2:1, and 5:1) and ramp rate of pyrolysis (5, 10, 20 and 30 °C/min) on NRG formation were investigated. If one parameter was regulated, the other parameters were identical to the as-prepared NRG-ME (2:1, 900 °C and 10 °C/min). The samples prepared at 700, 800, 900 and 1000 °C were donated as NRG-700, NRG-800, NRG-

45  900 (ME) and NRG-1000, respectively. The samples prepared with mass ratio of 1:1, 2:1 and

46  5:1 were donated as NRG-1:1, NRG-2:1 (ME) and NRG-5:1, respectively. The samples

47  prepared with the ramp rate of 5, 10, 20 and 30 °C/min donated as NRG-5, NRG-10 (ME),

48  NRG-20 and NRG-30, respectively.

49  Preparation of ZnNCN: Pure ZnNCN was synthesized based on other report.[1]

50  Specifically, 12.0 g $ZnCl_2$ was dissolved into 90 mL $H_2O$ under magnetic stirring.

51  Subsequently, 12.5% ammonia solution was added dropwise into the above solution until the

52  formation of white precipitate. Then, 25% ammonia solution was added to dissolve the

53  precipitate. Followingly, 60 mL cyanamide solution (0.1 g/mL) was added into the above

54  zinc-containing solution. After 3 h reaction, the white precipitate was filtered, washed with

55  water and dried at 60 °C for 12 h to obtain ZnNCN.

56  Measurement and Instruments: The phase structures of all samples were investigated on

57  a Philips/X' Pert PRO X-ray powder diffractometer (XRD) using CuKα radiation (λ=1.5418

58  Å). The surface functional groups were detected by Fourier transform infrared (FT-IR) spectra

59  conducted on a Bruker VERTEX70 spectrometer with a KBr beam splitter. The Raman data

60  were measured on a LabRAM HR800 Raman spectrometer using the excitation wavelength of

61  532 nm. The morphologies of materials were characterized by a NanoSEM 450 scanning

62  electron microscope (SEM) with accelerating voltage of 10 kV. The structural texture and

63  element distribution were observed by a JEM-2100F field-emission transmission electron

64  microscope (TEM) equipped with an energy-dispersive X-ray spectroscopy (EDX). The

65  chemical information of materials was measured using X-ray photoelectron spectroscopy

66  (XPS) conducted on a Kratos/Axis Ultra DLD-600 W spectrometer. Brunauer-Emmett-Teller

67 (BET) surface area of the obtained materials was collected by a Micro meritics ASAP 2020M

68 surface area analyzer with nitrogen adsorption at -196 °C. The reactive oxidative species

69 (ROSs) were investigated by electron paramagnetic resonance (EPR) on a Bruker A300

70 spectrometer using DMPO and TEMP as trapping agents.

71       Degradation performance of NRG samples: The catalytic degradation was carried out in

72 a 250 mL beaker which contained 200 mL of 20 mg/L tetracycline solution and 4 mg of NRG.

73 After adding 0.5 mL of fresh PMS (48 mg/mL) solution into the mixture, the degradation

74 reaction was initiated. About 3 mL of mixture was taken out and filtered through a 0.22 μm

75 pore-size syringe at different time intervals to detect the concentration of residual organics.

76 The concentrations of tetracycline was analyzed by high performance liquid chromatography-

77 mass spectrometry (HPLC, Agilent, 1260-Infinity) at a detection wavelength of 368 nm.[2]

78 Selected quenching agents (EtOH, $p$BZQ and FFA) were used to identify the reactive

79 oxidative species (ROS) generated in the reaction process. The degradation process was fitted

80 by the first-order kinetic model, obeying the following formula (Eq.1):

81
$$\ln\left(\frac{C}{C_0}\right) = -kt \qquad (1)$$

82 Where $C_0$ is the initial tetracycline concentration, $C$ is the concentration at a certain time t

83 during the degradation, and $k$ is the reaction rate constant.

84       Density functional theory (DFT) calculations: Adsorption of PMS on different N-doped

85 graphene was calculated via DFT based on a $C_{42}H_{16}$ model for pristine graphene. Vienna ab-

86 initio simulation package (VASP) was used to carried out calculations with the perdew-burke-

87 ernzerhof (PBE) exchange correlation functional.[3] DFT-D3 method was utilized to describe

88 van der Waals interactions.[4] The cut off energy was 400 eV and the interactions between the

4

89 atomic cores and electrons were described by the projector augmented wave (PAW) method.[5]

90 The sizes of unit cell for pyrrolic, pyridinic, and graphitic N-doped graphene were 25×25×15

91 Å, and all these structures were optimized until the force on each atom was less than 0.02

92 eV/Å. The Brillouin zone was only sampled by gamma point. (3×3×5) K-point was used to

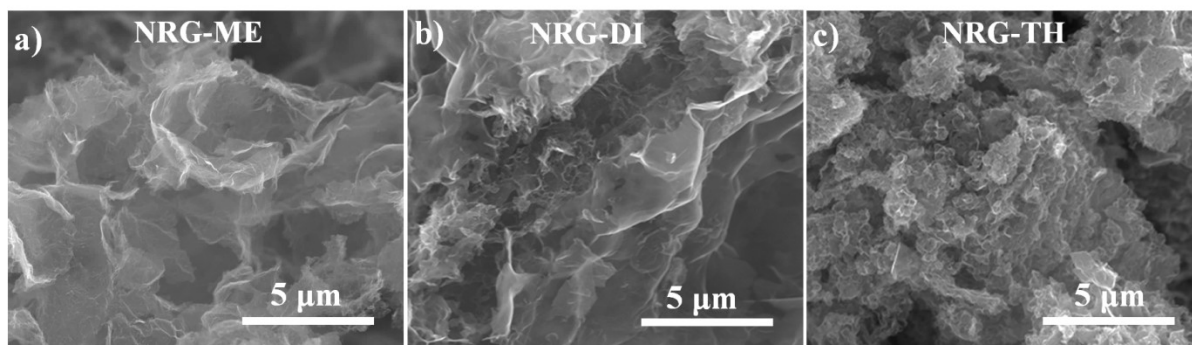93 calculate the electronic structures.
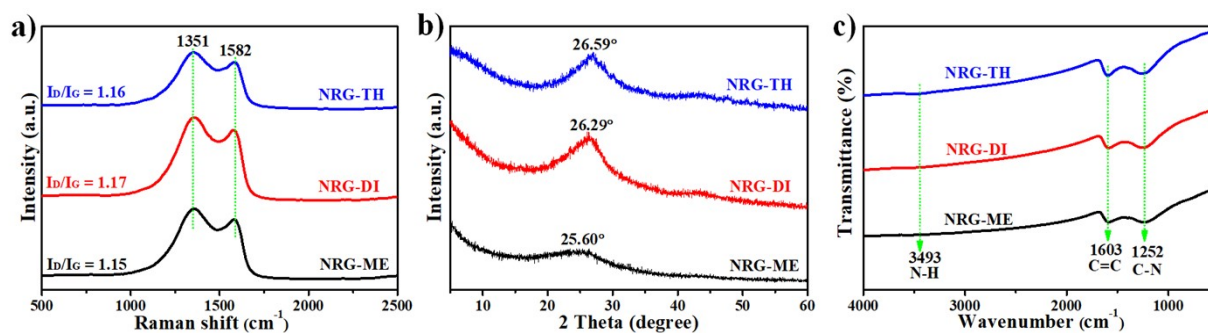
94

95

96

97

98

99

100

101

102

103

104

105

## S2 Supporting Figures



**Fig. S1.** SEM images of a) NRG-ME, b) NRG-DI and c) NRG-TH



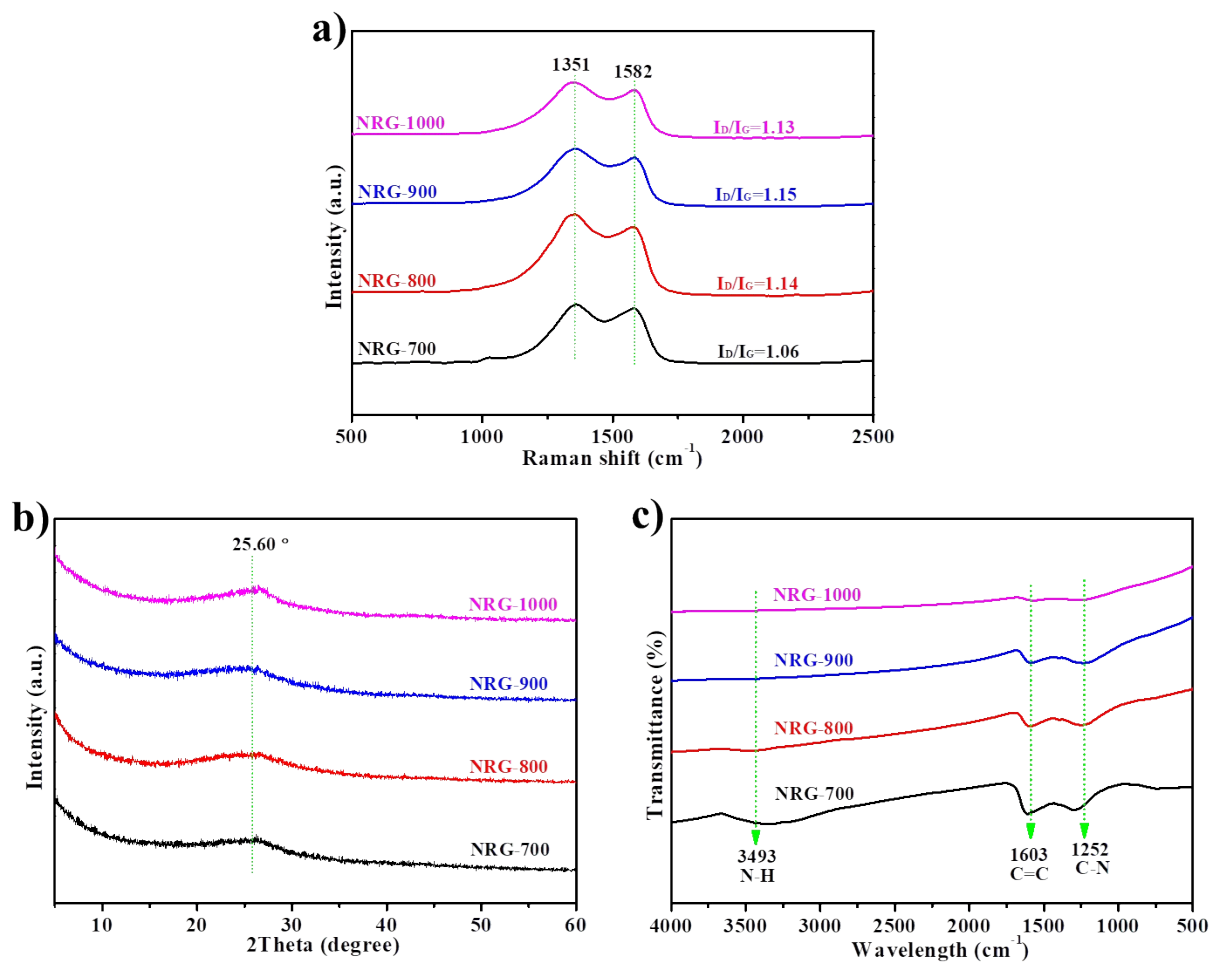**Fig. S2.** a) Raman spectra, b) XRD patterns and c) FT-IR spectra of NRG samples.
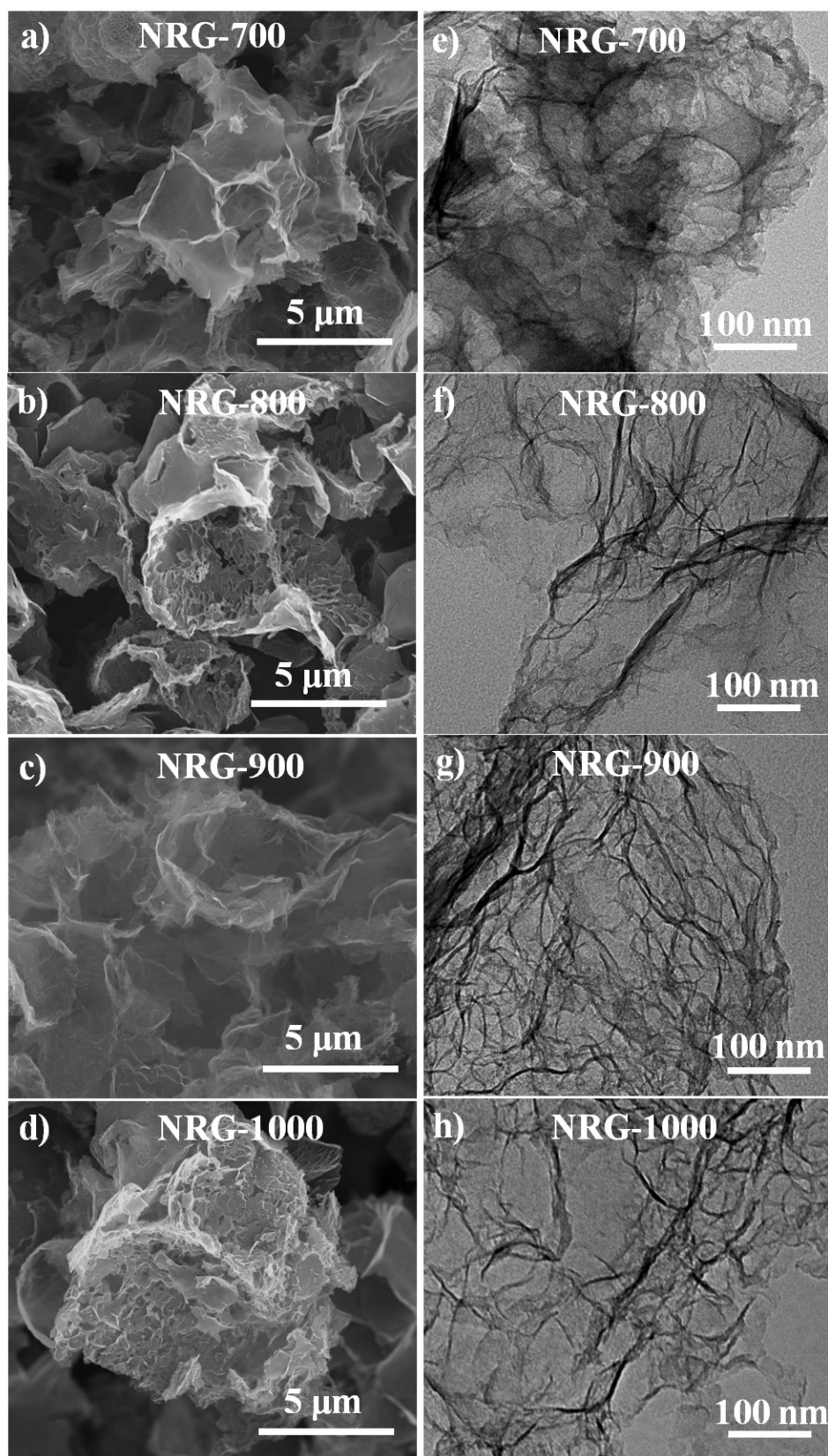
**Fig. S3.** a)-d) SEM images of NRG samples. e)-h) TEM images of NRG samples prepared at different temperature.

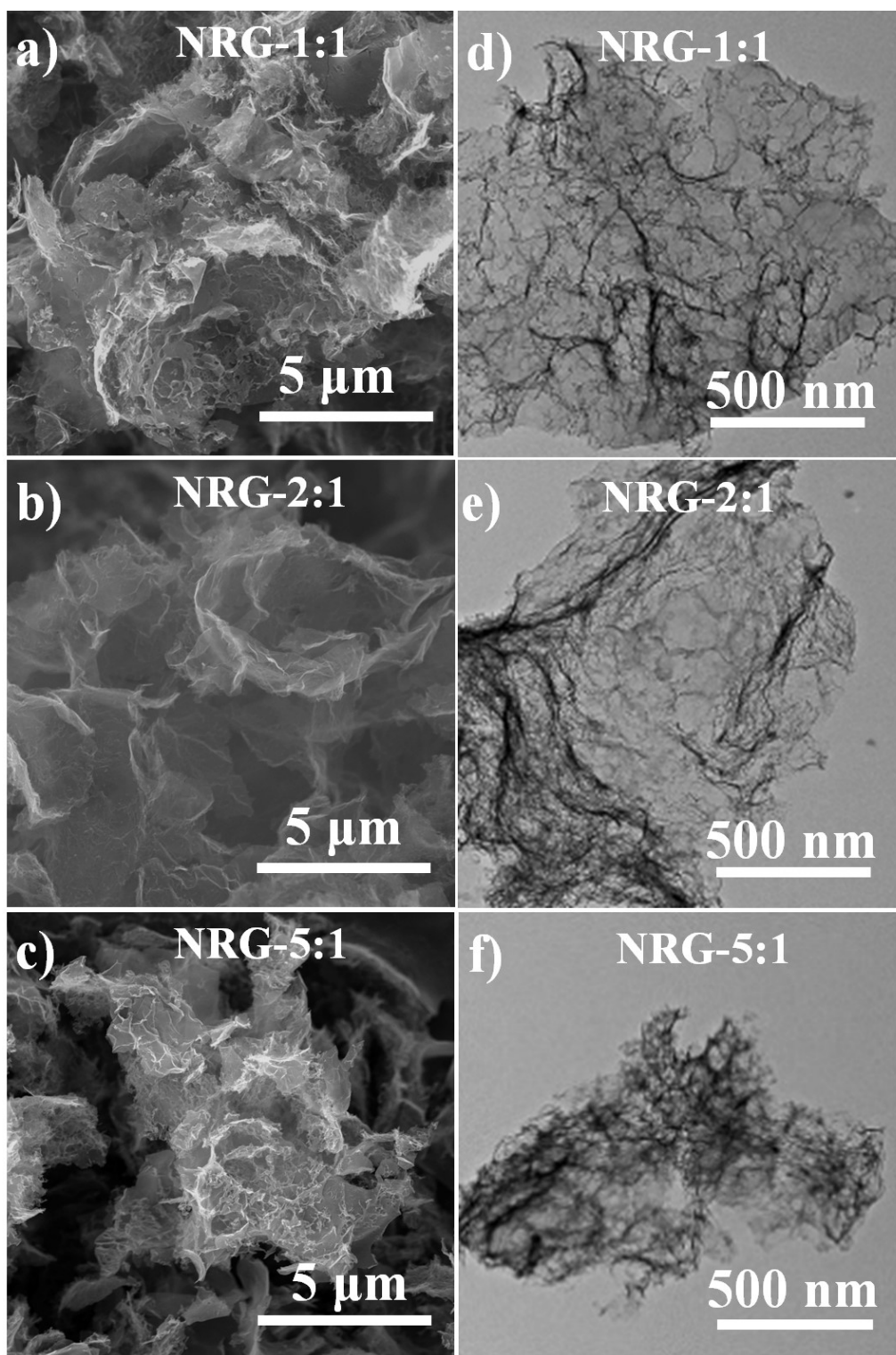**Fig. S4.** a) Raman spectra, b) XRD patterns and c) FT-IR spectra of NRG samples prepared at different temperature.

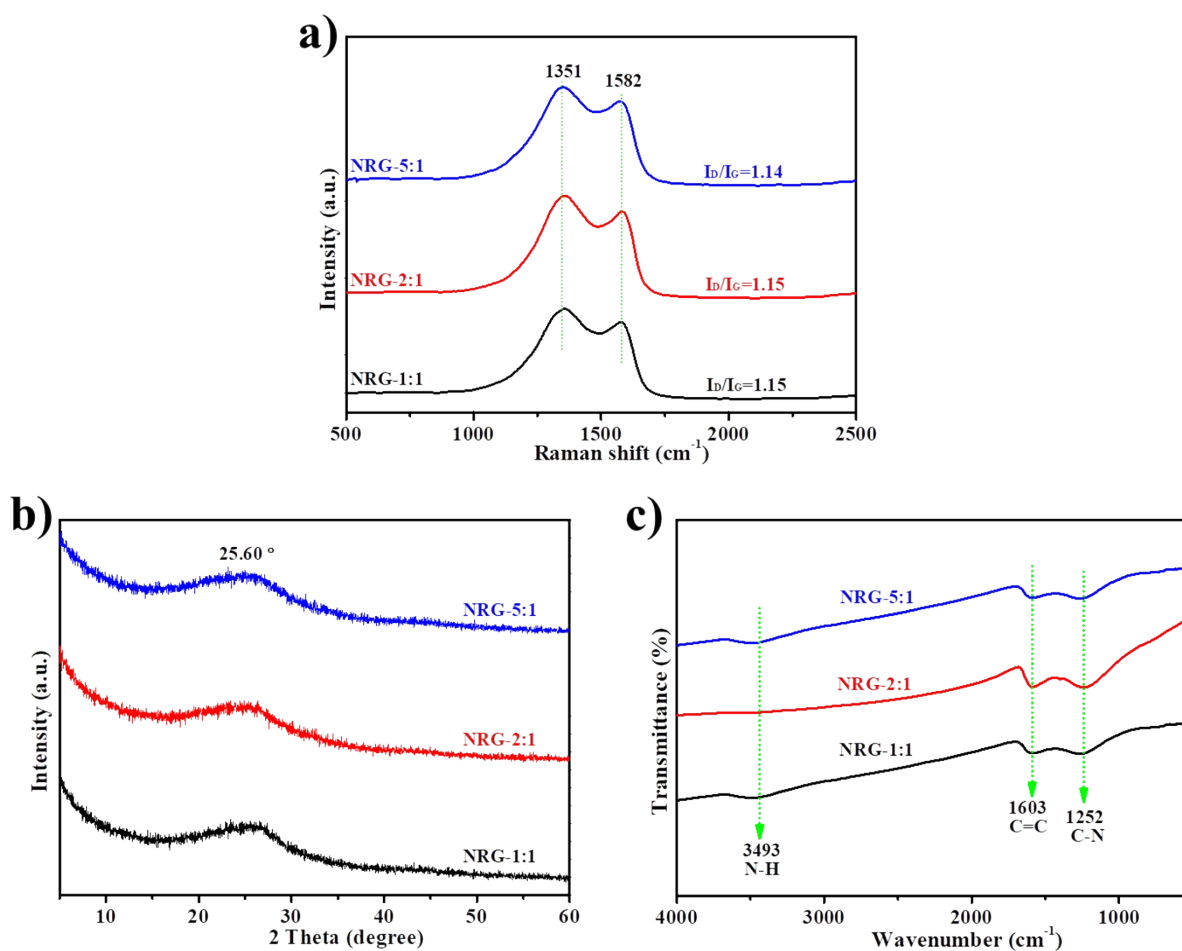**Fig. S5.** a-c) SEM images and d-f) TEM images of the products obtained at different melamine/Zn mass ratio.

**Fig. S6.** a) Raman spectra, b) XRD patterns and c) FT-IR spectra of NRG samples prepared at different melamine/Zn mass ratio.

141

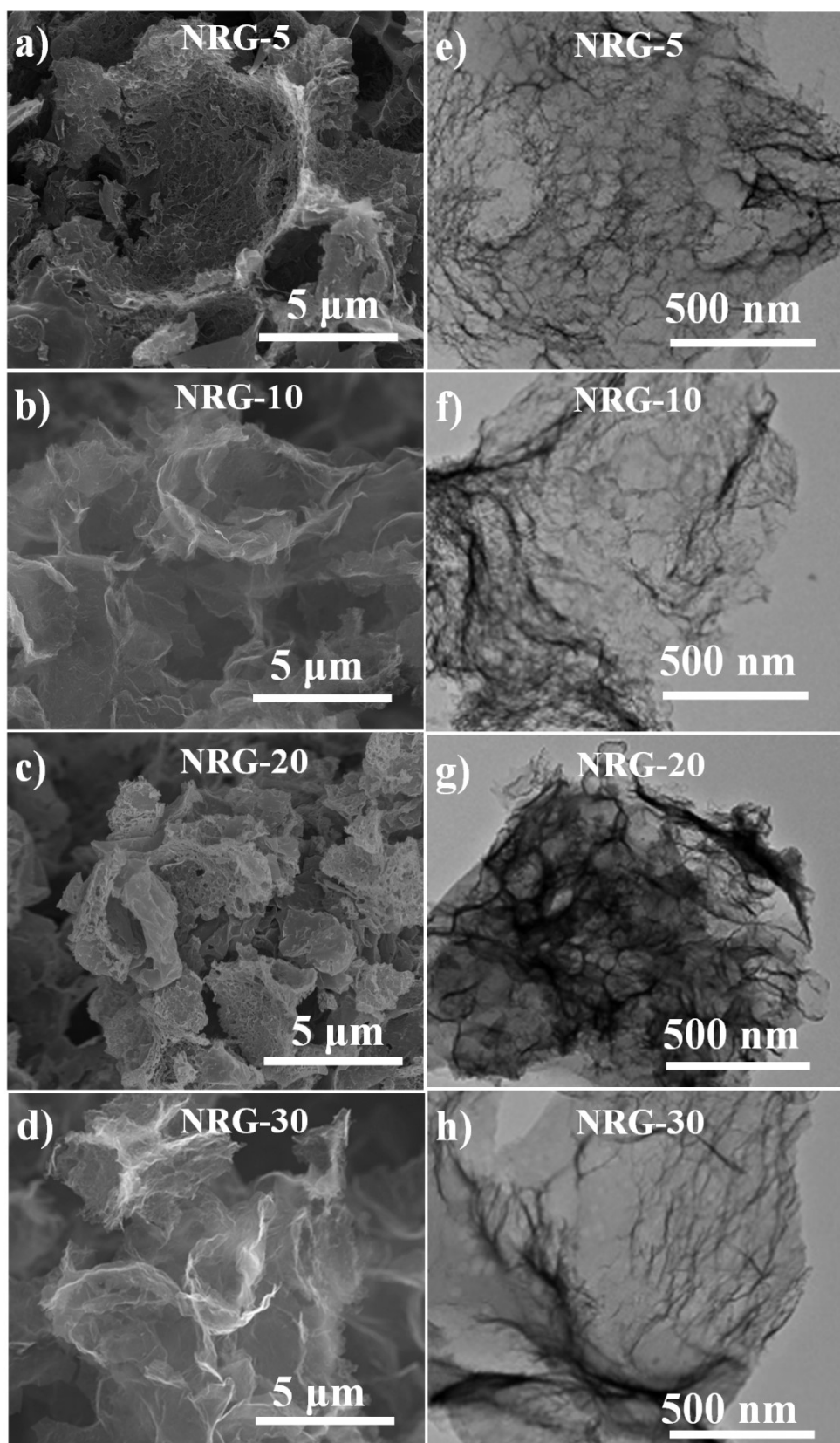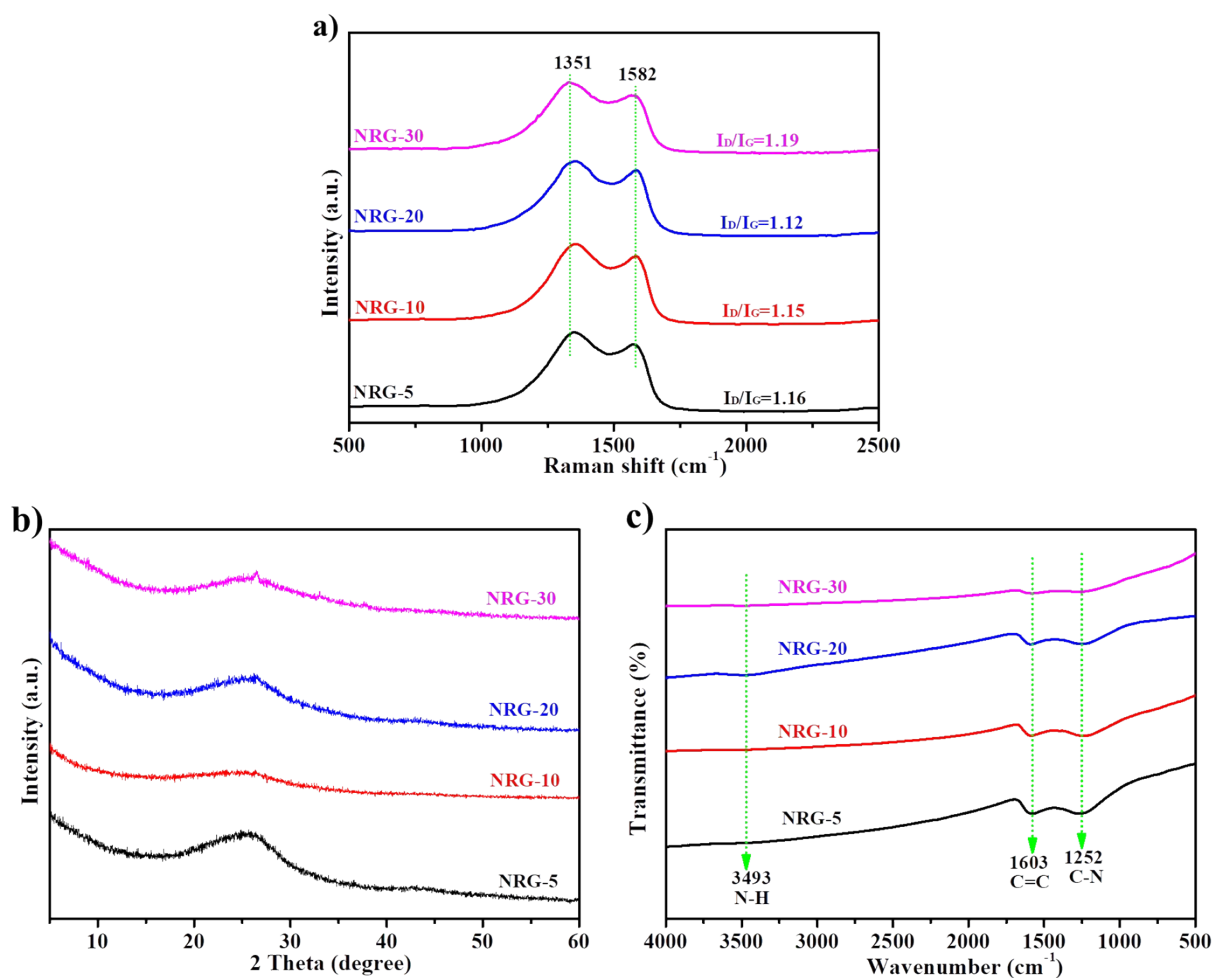**Fig. S7.** a-d) SEM images and e-h) TEM images of the products obtained at different ramp

rate.

**Fig. S8.** a) Raman spectra, b) XRD patterns and c) FT-IR spectra of NRG samples prepared at

different ramp rate.

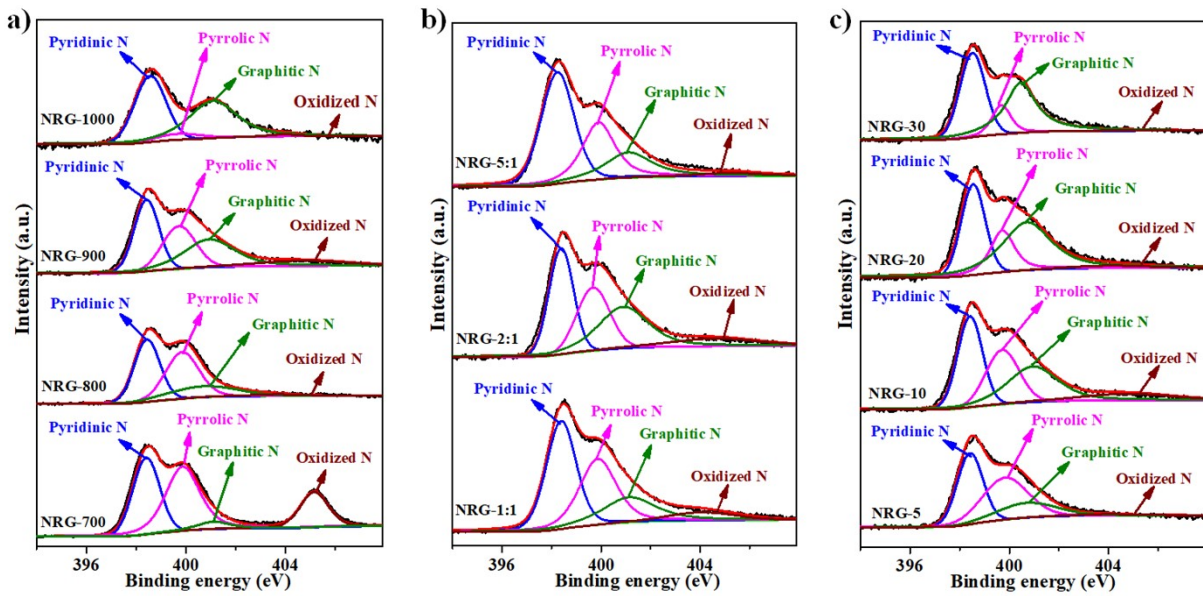**Fig. S9.** High-resolution N 1s XPS spectra of NRG samples prepared at different conditions: a) temperature, b) melamine/Zn mass ratio and c) ramp rate.
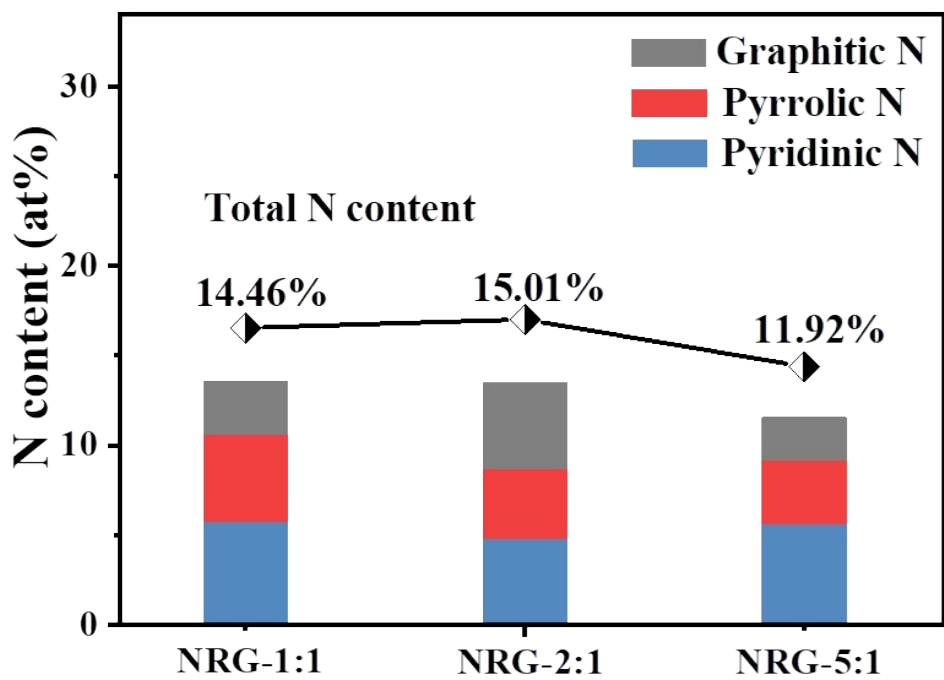
**Fig. S10.** N contents of NRG prepared at different melamine/Zn mass ratio.
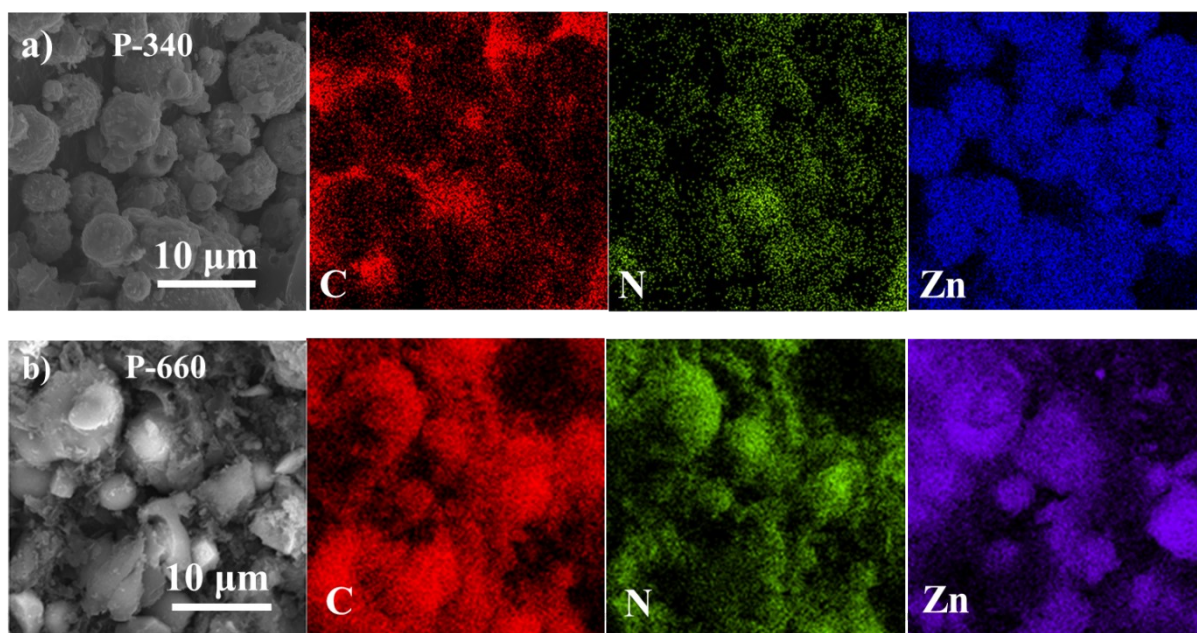
179

Fig. S11. EDX mappings of a) P-340 and b) P-660.

180

181

182

183

184

185

186

187

188
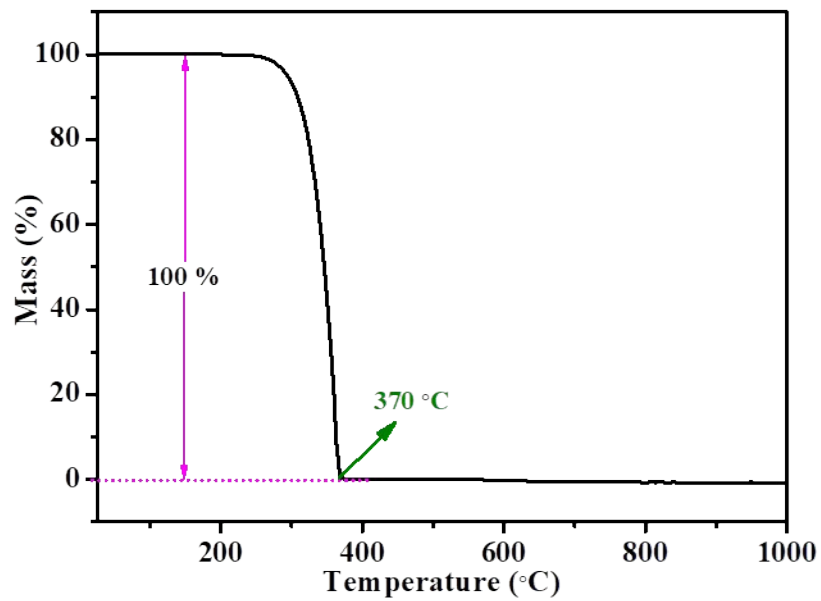
**Fig. S12.** TG curve during the pyrolysis of melamine.

189

190

191

192

193

194

195

196

197

198

199

200

201

202

203

204
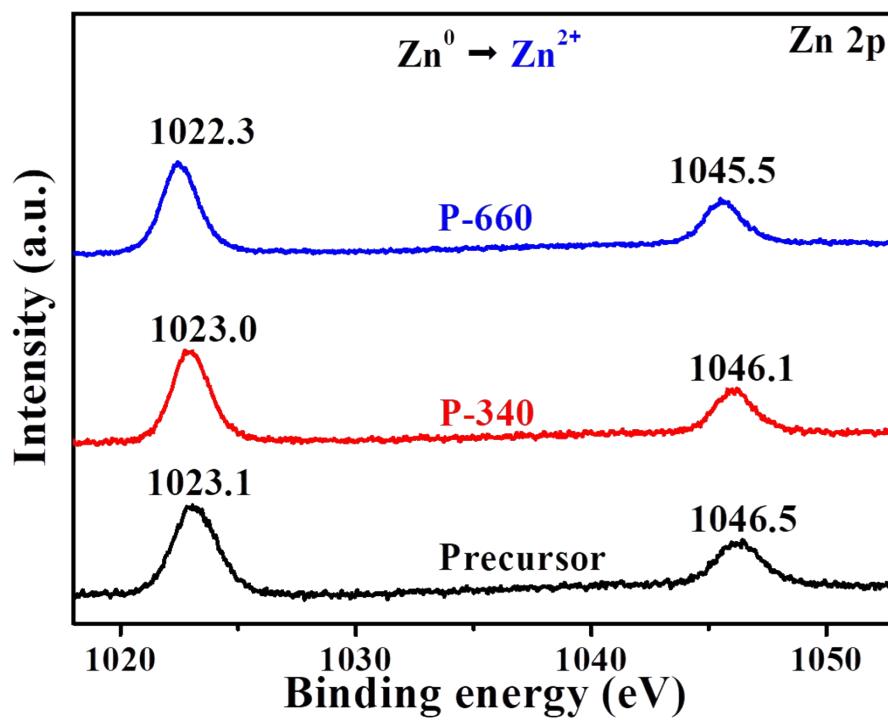
**Fig. S13.** High resolution Zn 2p XPS spectra of different P-T products.

a)

b)
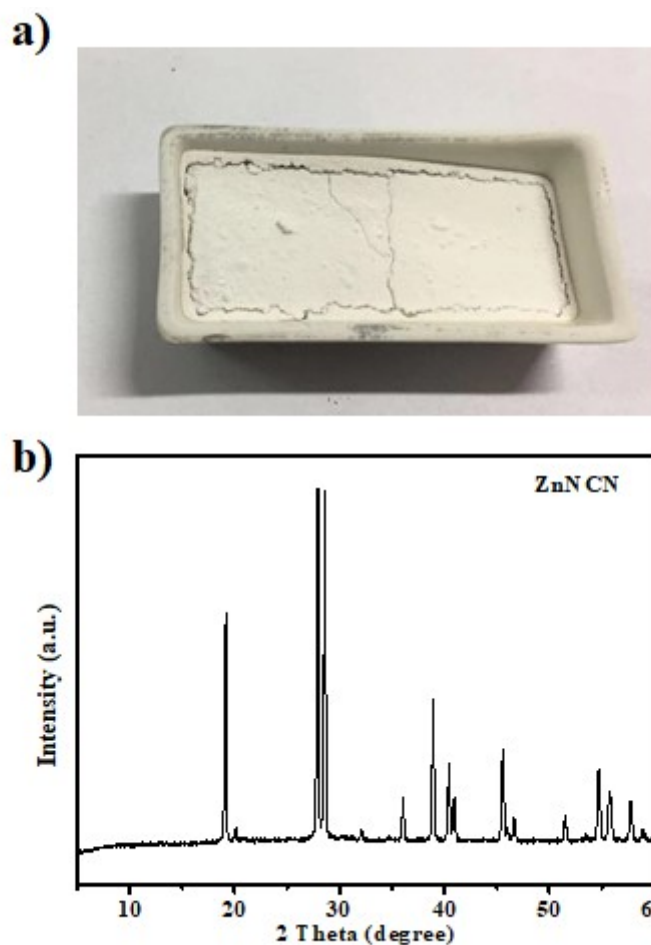
ZnN CN

**Fig. S14.** a) Photo image and b) XRD pattern of the product obtained by annealing the

mechanical mixture of ZnNCN and melamine with a mass ratio of 1:2 under 900 °C and ramp

rate of 10 °C/min.
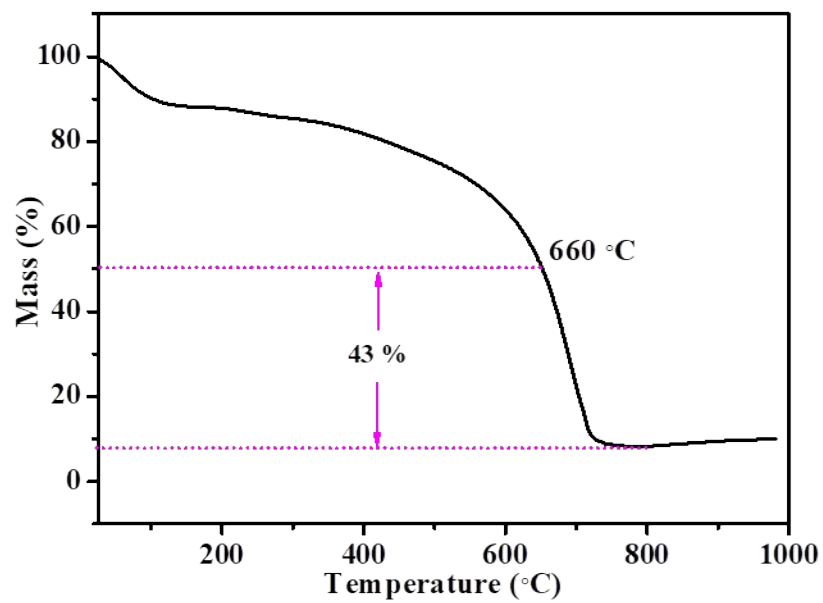
**Fig. S15.** TG curve during the pyrolysis of HCl-washed product of P-660.

dicyandiamide + Zn    after pyrolysis

thiourea + Zn    after pyrolysis

**Intensity (a.u.)**

**2 Theta (degree)**
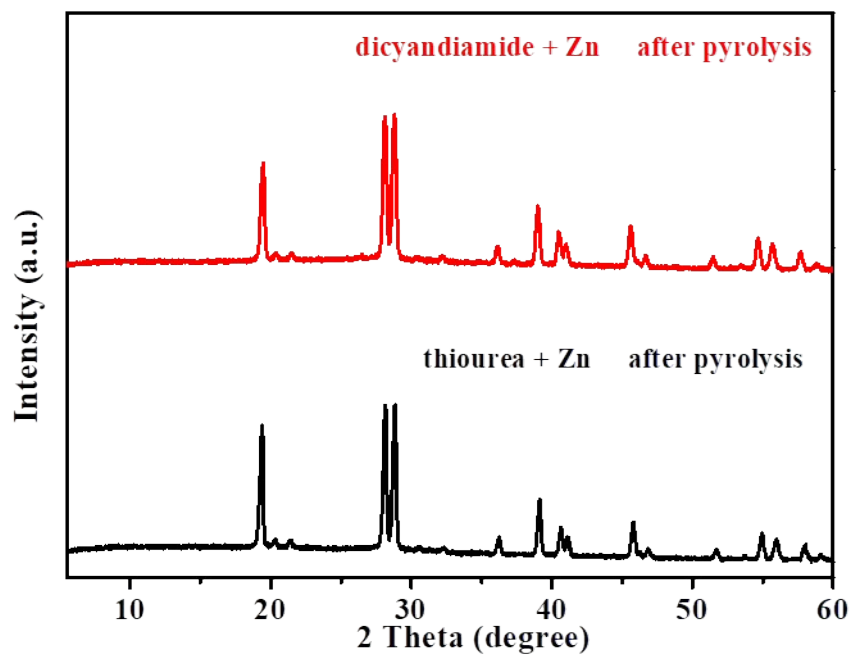
240

241    **Fig. S16.** XRD patterns of the pyrolytic products prepared by different organic precursors.

242

243
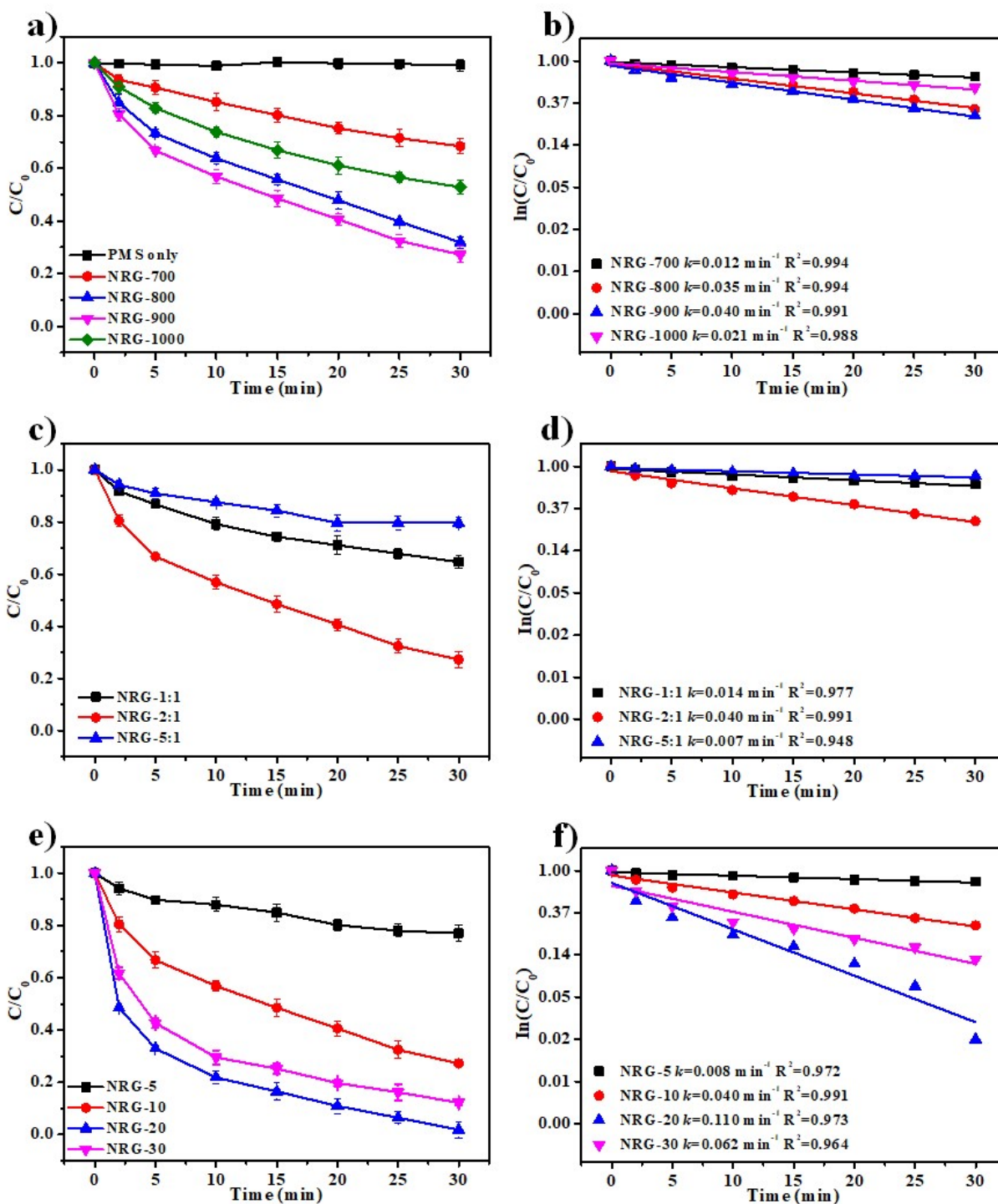
**Fig. S17.** Catalytic performance of tetracycline by different NRG samples and corresponding first-order kinetic curves (Condition: [PMS] = 0.2 mM, [tetracycline] = 20 mg/L, [NRG] = 20 mg/L).
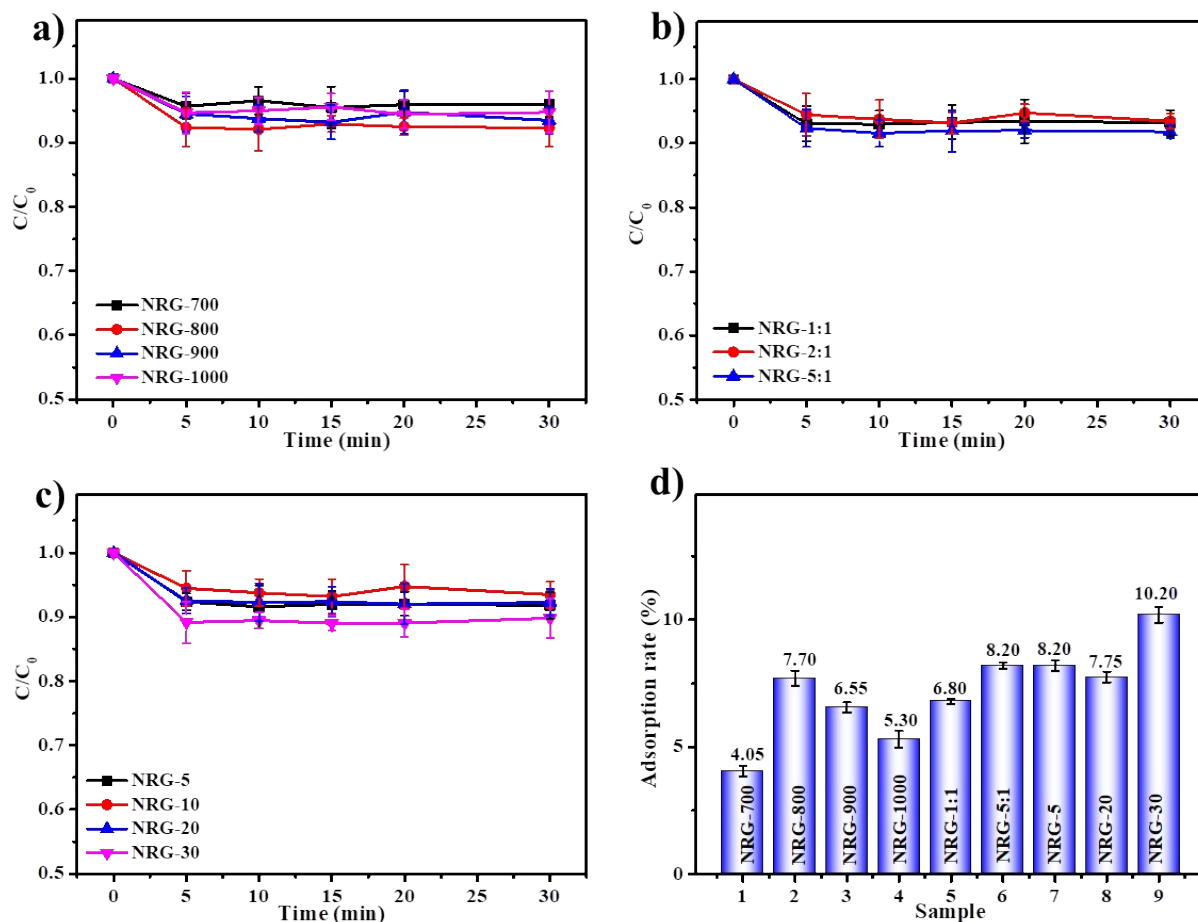
**Fig. S18.** Tetracycline adsorption rate of NRG samples (Condition: [tetracycline] = 20 mg/L,

[NRG] = 20 mg/L).
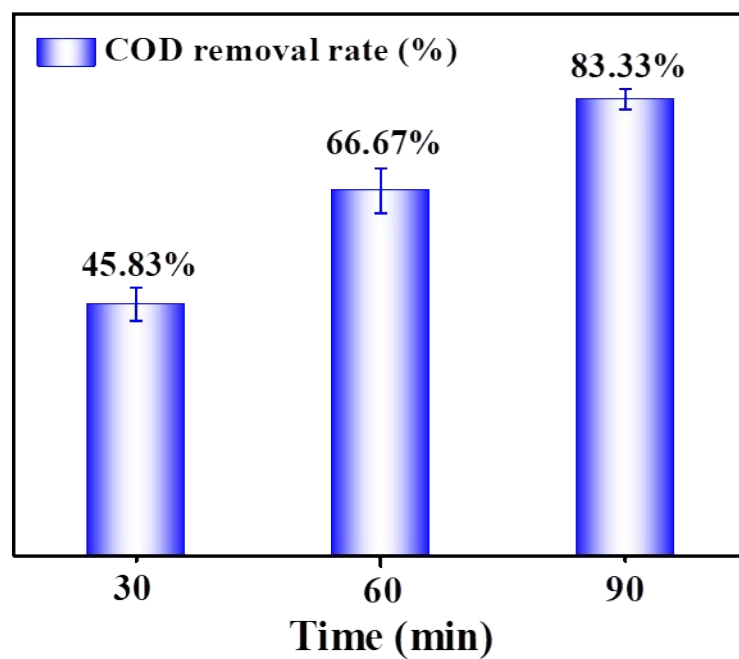
**Fig. S19.** COD removal rates of NRG-20/PMS system at different time.

261

262

263

264

265

266

267

268

269

270

271

272

273

274

275
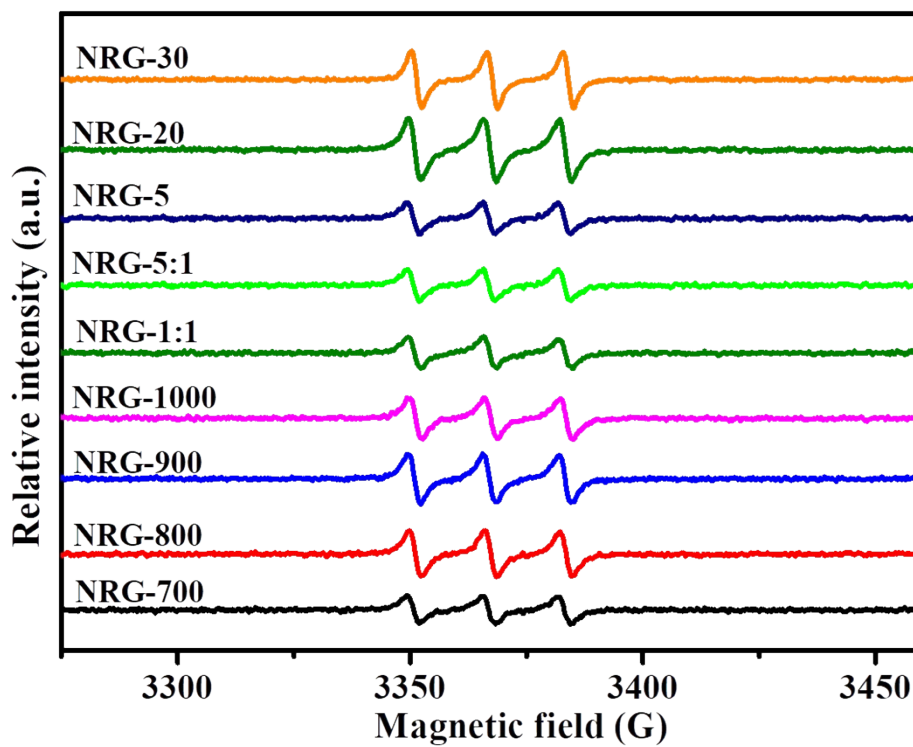
**Fig. S20.** EPR spectra of TEMP-$^1O_2$ in different NRG/PMS systems.

276

277

278

279

280

281

282

283

284

285

286

287

288
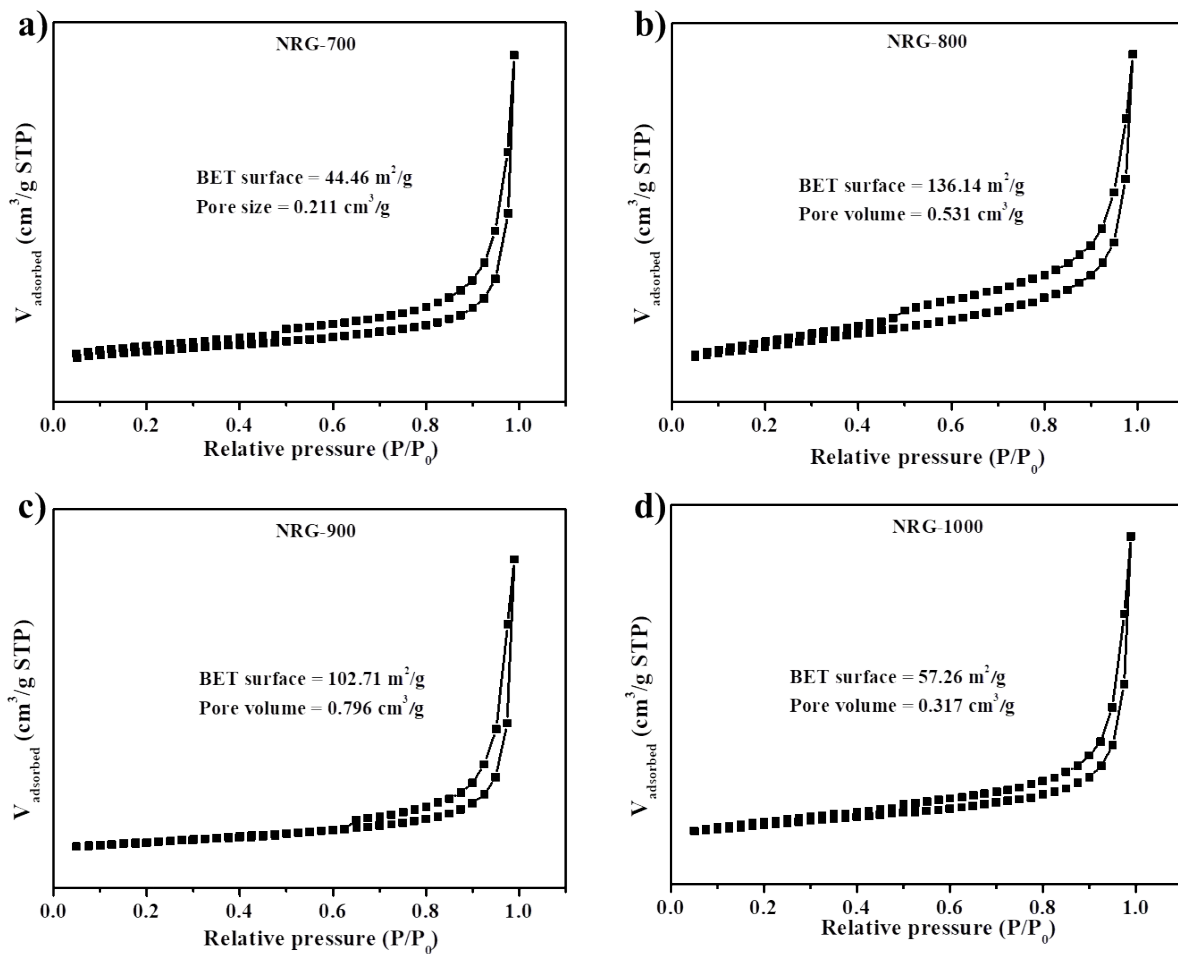
**Fig. S21.** $N_2$ adsorption-desorption isotherms of a) NRG-700, b) NRG-800, c) NRG-900 and d) NRG-1000 samples.

**a)** NRG-5

BET surface = 108.93 m$^2$/g
Pore volume = 0.959 cm$^3$/g

V$_{adsorbed}$ (cm$^3$/g STP)

Relative pressure (P/P$_0$)

**b)** NRG-10

BET surface = 102.71 m$^2$/g
Pore size = 0.796 cm$^3$/g

V$_{adsorbed}$ (cm$^3$/g STP)

Relative pressure (P/P$_0$)

**c)** NRG-20

BET surface = 124.04 m$^2$/g
Pore volume = 0.669 cm$^3$/g

V$_{adsorbed}$ (cm$^3$/g STP)

Relative pressure (P/P$_0$)

**d)** NRG-30

BET surface = 233.12 m$^2$/g
Pore volume = 1.445 cm$^3$/g

V$_{adsorbed}$ (cm$^3$/g STP)

Relative pressure (P/P$_0$)
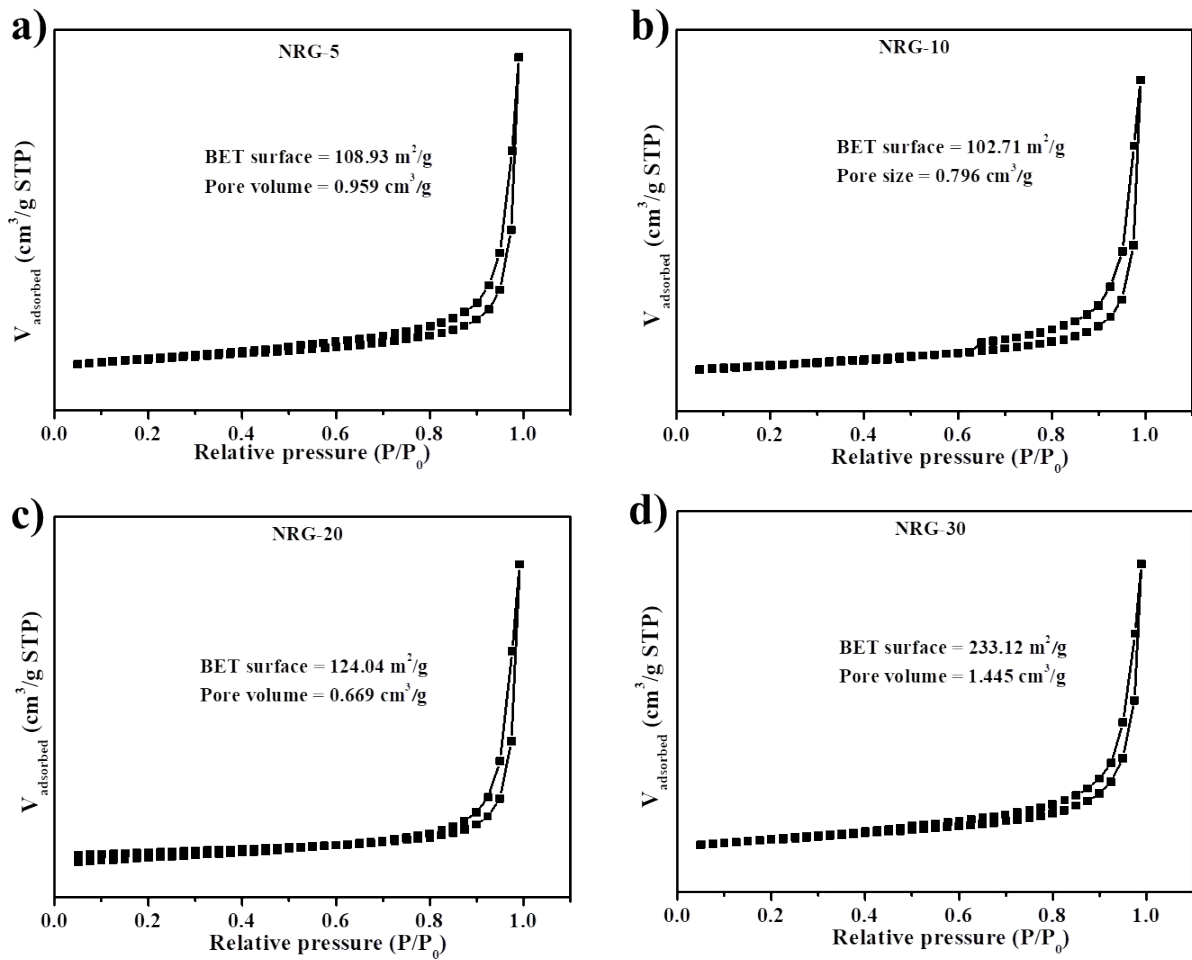
**Fig. S22.** N$_2$ adsorption-desorption isotherms of a) NRG-5, b) NRG-10, c) NRG-20 and d) NRG-30 samples.

a) NRG-1:1

BET surface = 113.43 $m^2$/g
Pore volume = 0.0.816 $cm^3$/g

V$_{adsorbed}$ (cm$^3$/g STP)

Relative pressure (P/P$_0$)

b) NRG-2:1

BET surface = 102.71 $m^2$/g
Pore volume = 0.796 $cm^3$/g

V$_{adsorbed}$ (cm$^3$/g STP)

Relative pressure (P/P$_0$)

c) NRG-5:1

BET surface = 39.25 $m^2$/g
Pore volume = 0.294 $cm^3$/g

V$_{adsorbed}$ (cm$^3$/g STP)
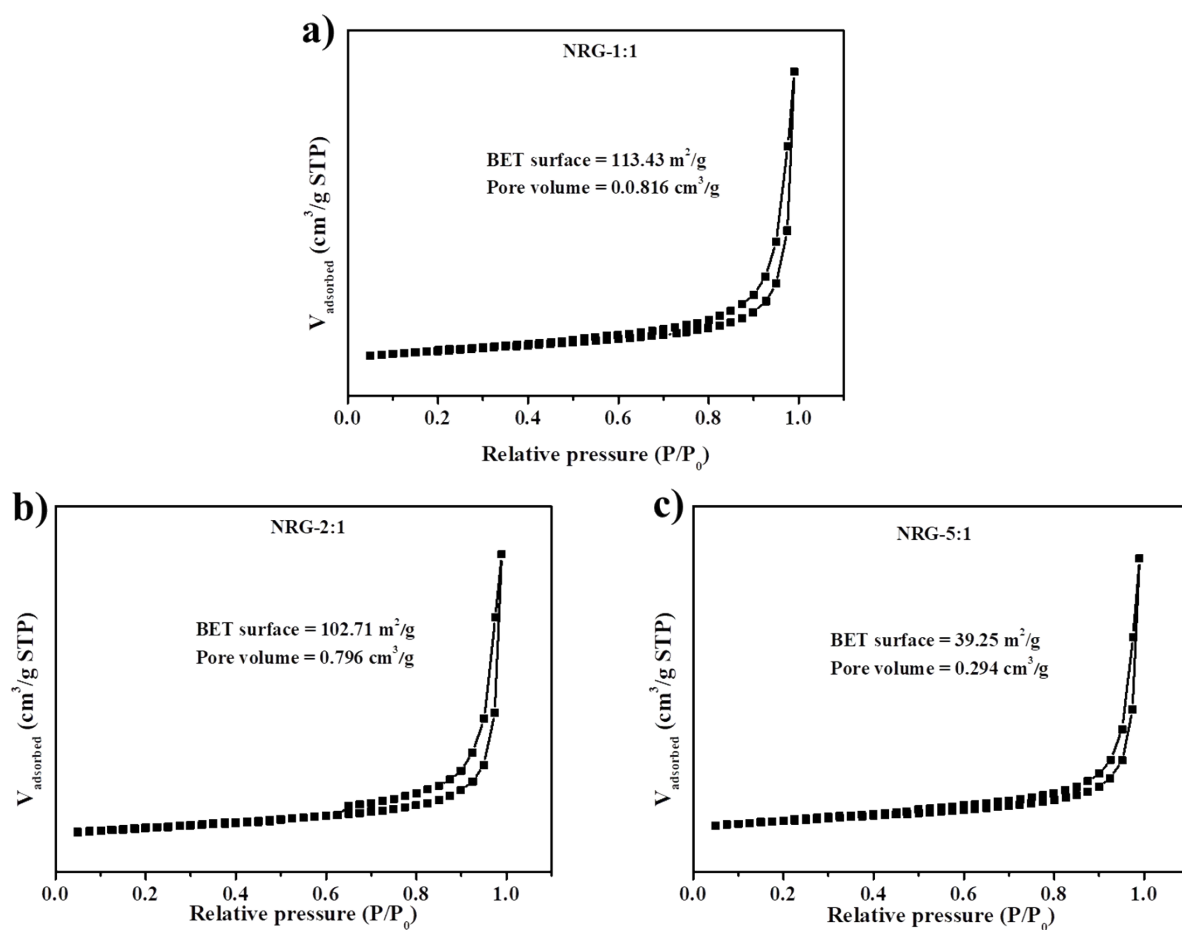
Relative pressure (P/P$_0$)

**Fig. S23.** $N_2$ adsorption-desorption isotherms of a) NRG-1:1, b) NRG-2:1 and c) NRG-5:1 samples.
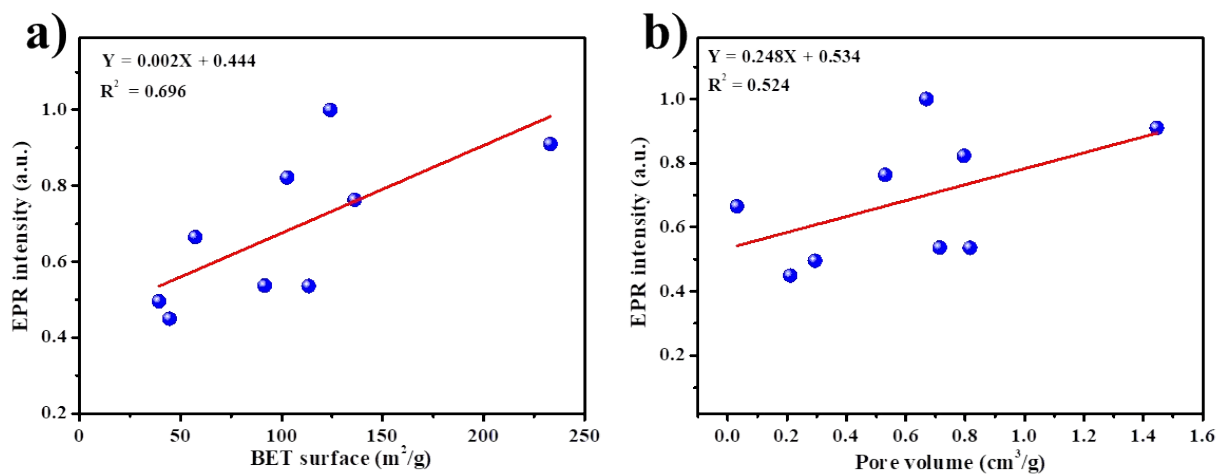
**Fig. S24.** a) BET surface and b) pore volume versus normalized TEMP-$^1O_2$ EPR intensity.

317

318

319

320

321

322

323

324

325

326

327

328

329

330
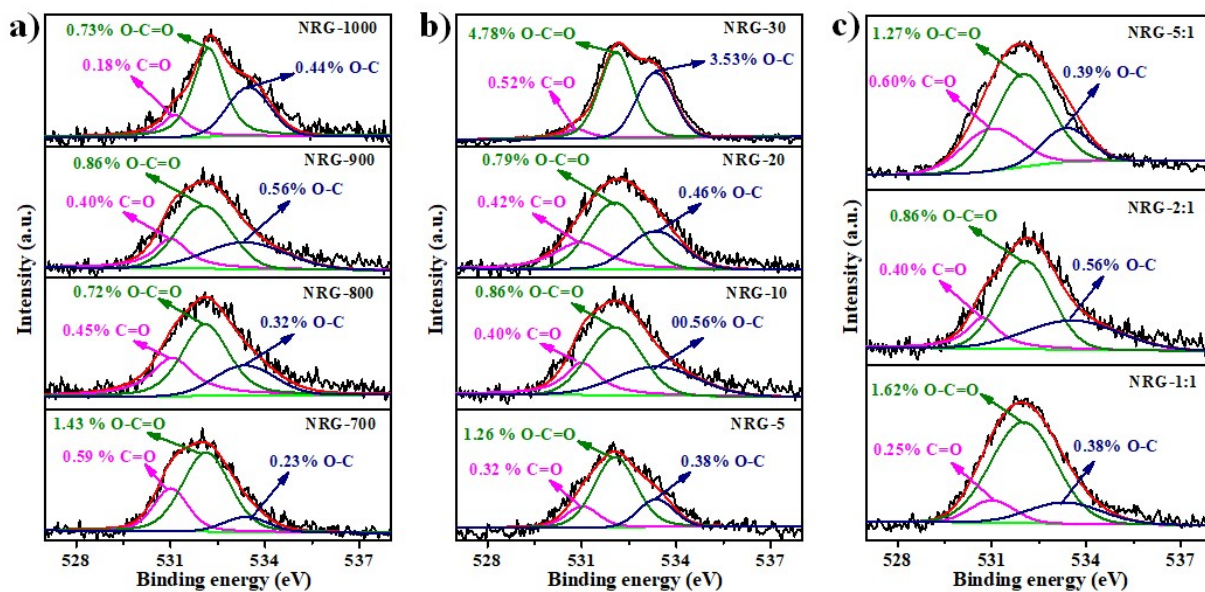
Fig. S25. High-resolution O 1s XPS spectra of NRG samples prepared at different conditions: a) annealing temperature, b) ramp rate and c) melamine/Zn mass ratio.
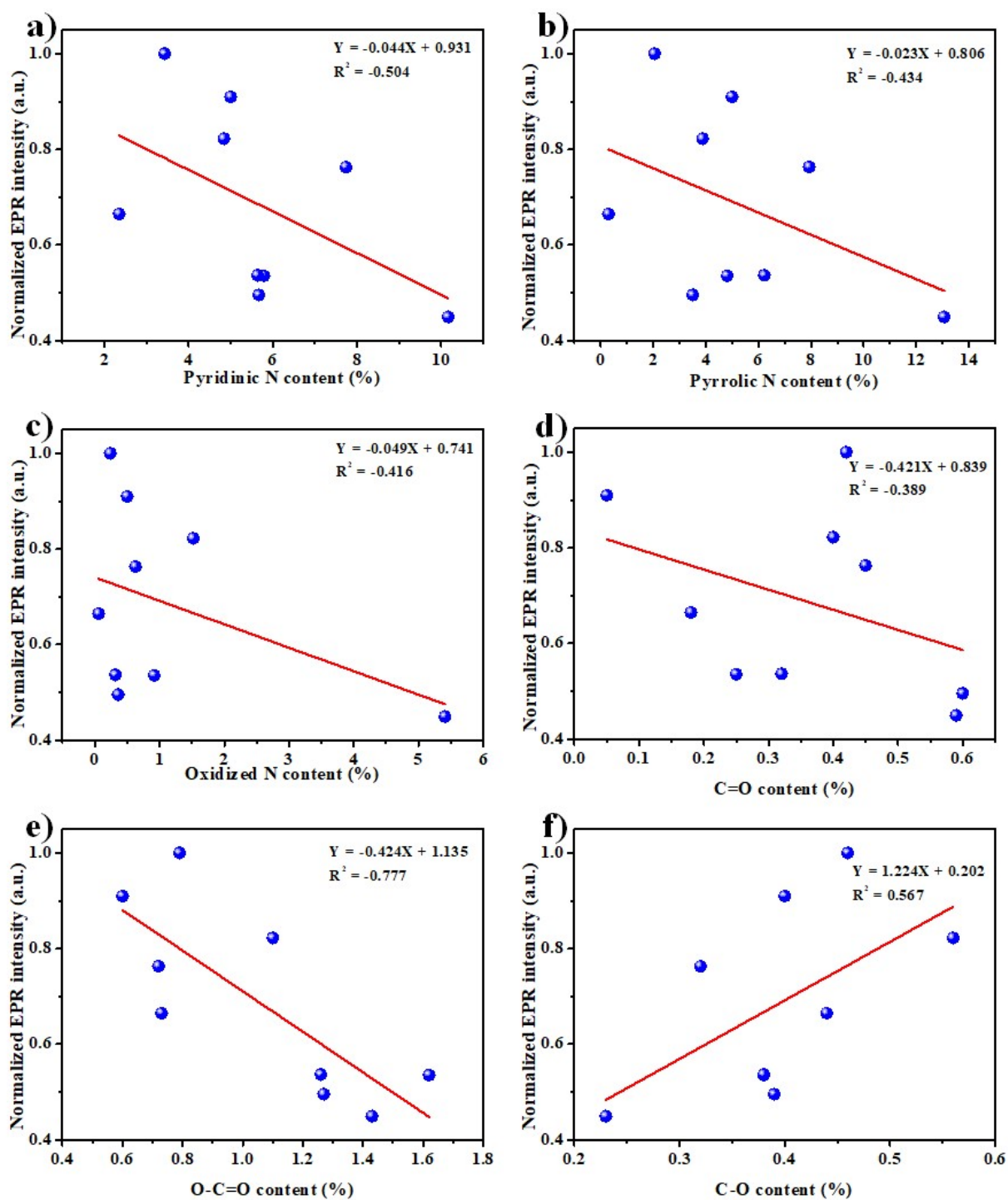
**Fig. S26.** a) pyridinic N, b) pyrrolic N, c) oxidized N, d) C=O, e) O-C=O and f) C-O amount

versus normalized TEMP-$^1O_2$ EPR intensity.

346

347

348

349

350

351

30
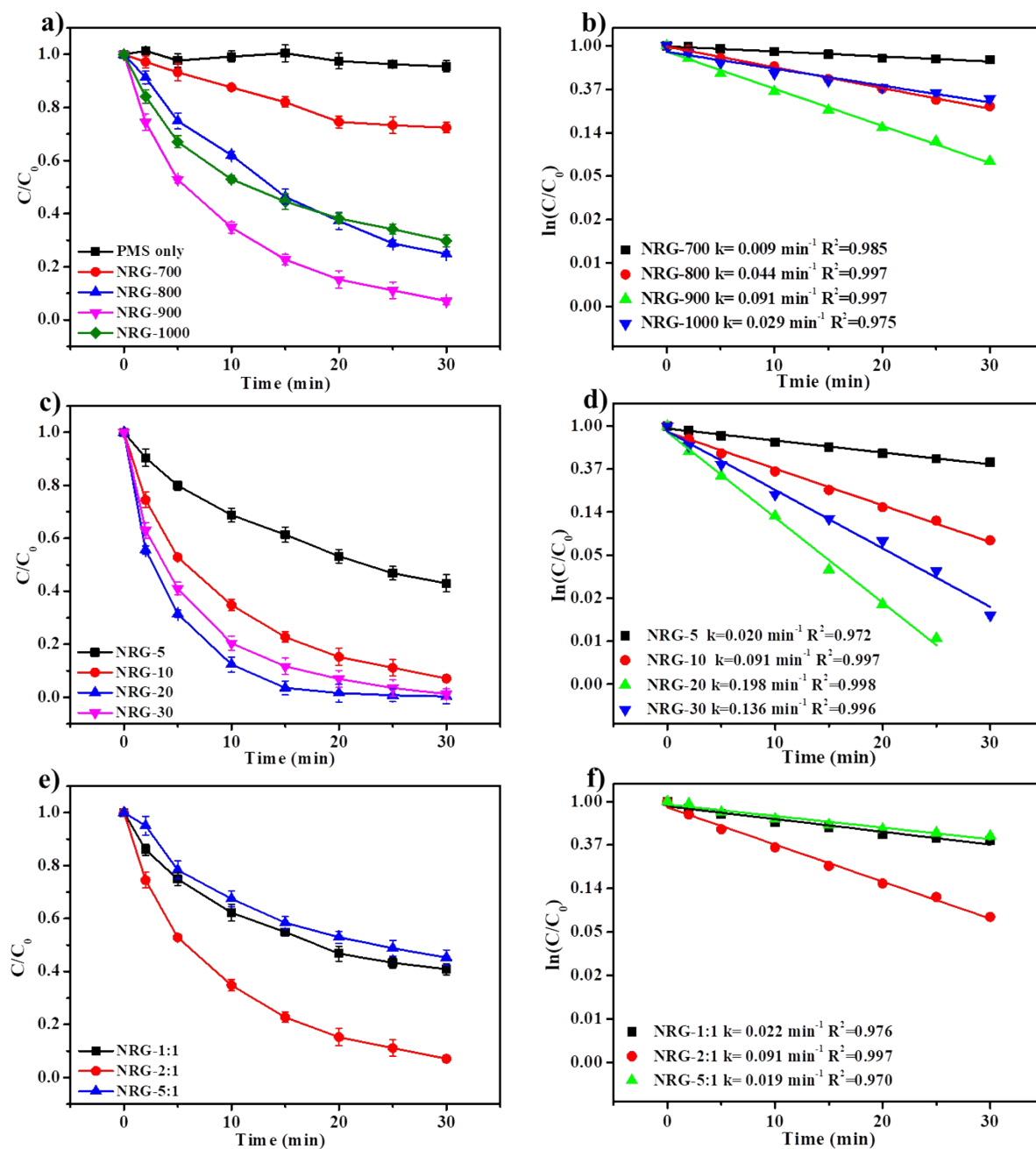
Fig. S27. a-f) Catalytic performance of RhB by different NRG samples and corresponding first-order kinetic curves (Condition: [PMS] = 0.2 mM, [RhB] = 20 mg/L, [NRG] = 20 mg/L).

352

353

354

355

356

357

358
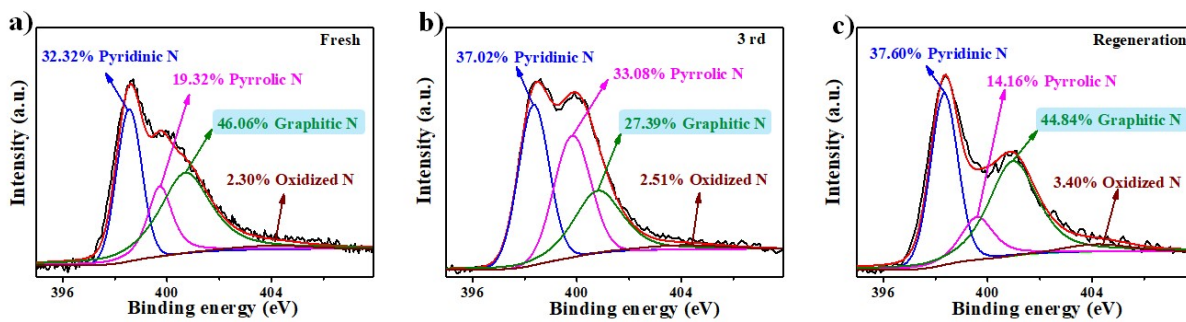
**Fig. S28.** High-resolution N 1s XPS spectra of a) fresh, b) used and c) regenerated NRG-20 samples.
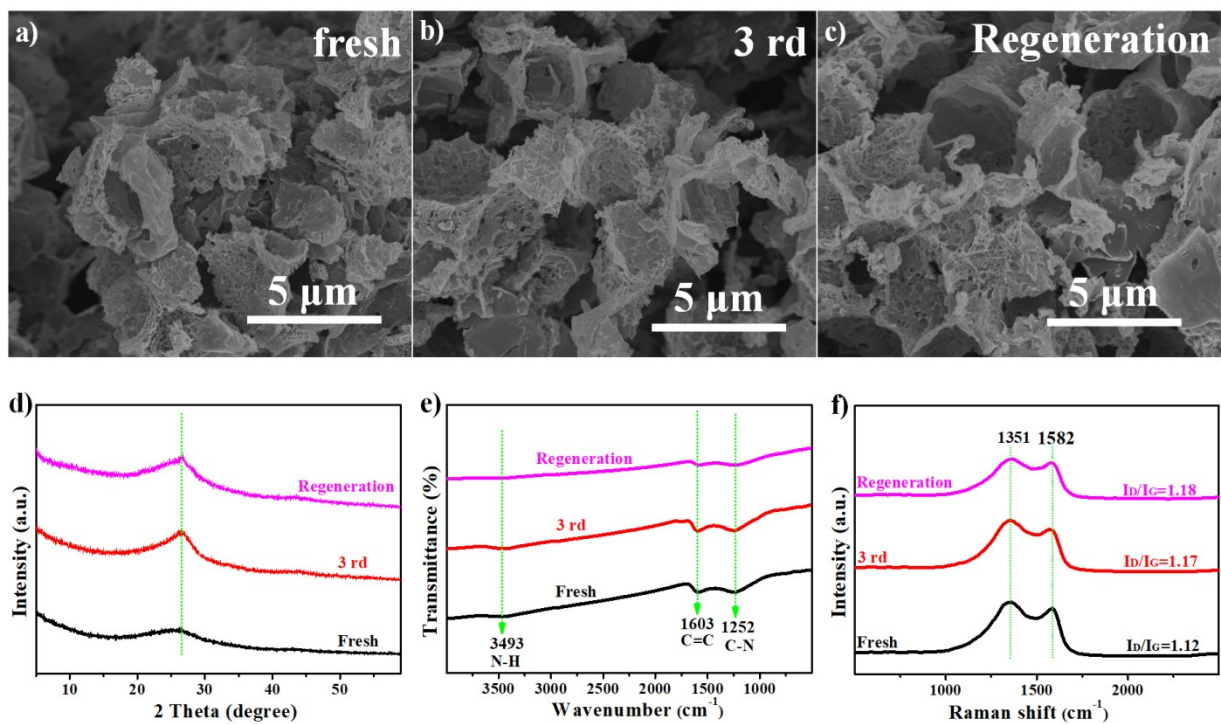
**Fig. S29.** a-c) SEM images, d) XRD patterns, e) FT-IR and f) Raman spectra of fresh, used and regenerated NRG-20 samples.
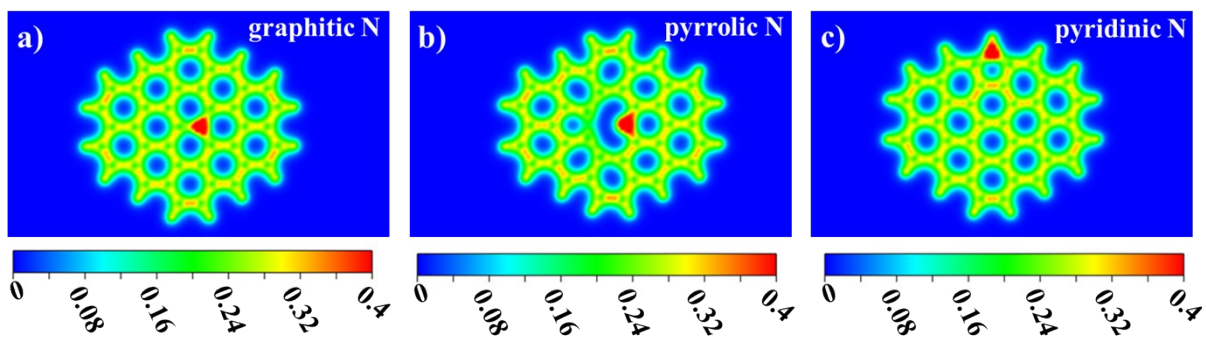
**Fig. S30**. a)-c) Valence-electron density maps of different N-doped graphene.

392

393

394

395

396

397

398

399

400

401

402

403
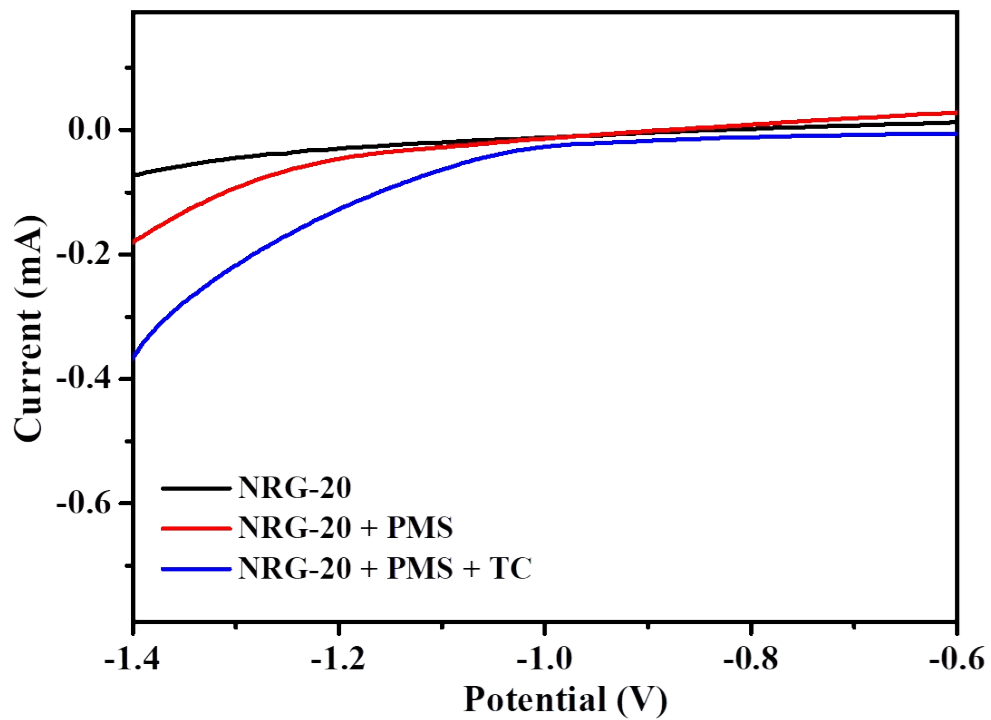
**Fig. S31.** LSV curves of NRG-20.

404

405

406

407

408

409

410

411

412

413

414

415

416

417

418　S3 Supporting Tables

419　**Table S1** Chemical properties of nitrogen-doped graphene prepared by different methods.

| Precursor | Material | Total N content (at%) | Method | Ref. |
|---|---|---|---|---|
| Ni/B/SiO$_2$/Si | NG | 0.95 | CVD | [6] |
| Ni$_{30}$Mn$_{70}$ + pyridine | NG | 1.10 | CVD | [7] |
| Acetonitrile | NG | 1.40 | CVD | [8] |
| Ni + benzene + pyridine | NS500 | 2.90 | CVD | [9] |
| Ni + CH$_4$ | NG | 2.00 | CVD | [10] |
| Azafullerence | NG | 1.80 | CVD | [11] |
| Graphene | NG | 1.35 | Plasma treatment | [12] |
| Graphene | NG | 1.00 | Ion implantation | [13] |
| NH$_3$ + pyridine + H$_2$ + He | NG | 1.40 | Arc discharge | [14] |
| g-C$_3$N$_4$ | NG | 0.70 | Ball milling | [15] |
| GO + NH$_3$ | NG | 5.00 | Prolysis | [16] |
| Triethylene glycol + Ni$_{30}$Mn$_{70}$ | N-MG-600 | 5.83 | Prolysis | [17] |
| GO + NH$_3$ | N-GF | 6.80 | Prolysis | [18] |
| GO + zinc gluconate + urea | N-C@G-900 | 4.20 | Prolysis | [19] |
| GO + cyanamide | C-NGNSs-900 | 9.90 | Prolysis | [20] |
| g-C$_3$N$_4$ + zinc | N-FLG-900 | 14.65 | Prolysis | [21] |
| Melamine | NRG-ME | 15.04 | Prolysis | This work |
| Dicyandiamide | NRG-DI | 13.63 | Prolysis | This work |
| Thiourea | NRG-TI | 14.33 | Prolysis | This work |

420

421

422

423

424

425

426

427

428 **Table S2** The catalytic performance comparison of recently reported catalysts for tetracycline

429 degradation. The turnover frequency (TOF) was calculated via dividing the reaction rate

430 constant of organics degradation by the catalyst concentration [22, 23].

| Catalyst amount (g/L) | tetracycline concentration (mg/L) | PMS/H$_2$O$_2$ amount (mM) | Remove efficiency | TOF (g$^{-1}$•min$^{-1}$) | Ref. |
|---|---|---|---|---|---|
| FeSe$_2$ (0.1) | 20 | PMS (0.1) | 82% (120 min) | / | [24] |
| H-450CoMnO$_x$@NC (0.1) | 13 | PMS (0.3) | 88.9% (30 min) | 1.83 | [25] |
| CuFeO2/BC-1.0 (0.5) | 20 | H$_2$O$_2$ (50) | 88.4 % (300 min) | 0.01 | [26] |
| PGBF-N (0.1) | 20 | PMS (1.0) | 96.5% (150 min) | 0.02 | [27] |
| C@FONC (0.5) | 150 | H$_2$O$_2$ (5.0) | 97.0% (120 min) | 0.01 | [28] |
| Fe/O-dopedg-C$_3$N$_4$ (0.1) | 10 | PMS (1.0) | 95% (6 min) | / | [29] |
| 5%Ca-Fe$_2$O$_3$ (0.5) | 10 | PMS (3.3) | 95% (120 min) | / | [30] |
| α-FeOOH-HA (1.0) | 20 | H$_2$O$_2$ (1.0) | 98% (30 min) | 0.12 | [31] |
| SOH-600 (0.15) | 50 | H$_2$O$_2$ (1.6) | 80% (240 min) | 0.03 | [32] |
| □Fe$_3$(HITP)$_2$ (0.4) | 20 | H$_2$O$_2$ (40.0) | 96.7% (30 min) | / | [33] |
| □CNF-4 (0.5) | 21 | / | 64.2% (70 min) | 0.03 | [34] |
| □AgI(5%)/CeO$_2$ (0.3) | 40 | / | 88.1% (180 min) | 0.03 | [35] |
| □□CTOC/BaTiO$_3$/CuS (0.2) | 10 | / | 100% (60 min) | 0.44 | [36] |
| □1.0 %CTQDs/BWO (0.05) | 20 | / | 91.5% (135 min) | 0.29 | [37] |
| □CALTCT-15 (1.0) | 10 | / | 96.7% (60 min) | 0.05 | [38] |
| □Ag/Ag$_3$PO$_4$/BiVO$_4$/RGO(0.05) | 10 | / | 95.0% (60 min) | / | [39] |
| □3D-PDI (0.5) | 20 | / | 80% (150 min) | 0.02 | [40] |
| □ZIS@P20 (0.2) | 20 | / | 99.9% (60 min) | 0.04 | [41] |
| □CuS$_4$-ZIS (0.5) | 20 | / | 90% (40 min) | 0.12 | [42] |
| NRG-20 (0.02) | 20 | PMS (0.1) | 98.2% (30 min) | 5.50 | This work |

431 □represents that the reaction was carried out under light irradiation.

432

433

434

435

436    **Table S3** Amount of different N configurations in NRG samples.

| Sample | $N_{py}/N_T$ (%) | $N_{py}/N_T$ (%) | $N_g/N_T$ (%) | $N_o/N_T$ (%) | $N_{py}$ (at%) | $N_{pr}$ (at%) | $N_g$ (at%) | $N_o$ (at%) |
|---|---|---|---|---|---|---|---|---|
| NRG-ME | 32.26 | 25.84 | 31.79 | 10.11 | 4.84 | 3.88 | 4.77 | 1.52 |
| NRG-DI | 43.93 | 19.60 | 31.12 | 5.35 | 5.99 | 2.67 | 4.24 | 0.73 |
| NRG-TI | 39.07 | 37.85 | 16.18 | 6.90 | 5.60 | 5.42 | 2.32 | 0.99 |
| NRG-700 | 33.59 | 43.12 | 5.42 | 17.88 | 10.17 | 13.06 | 1.64 | 5.41 |
| NRG-800 | 38.75 | 39.68 | 18.43 | 3.14 | 7.74 | 7.93 | 3.68 | 0.63 |
| NRG-900 | 32.26 | 25.84 | 31.79 | 10.11 | 4.84 | 3.88 | 4.77 | 1.52 |
| NRG-1000 | 44.34 | 5.70 | 48.79 | 1.17 | 2.35 | 0.30 | 2.59 | 0.06 |
| NRG-1:1 | 40.02 | 33.28 | 20.36 | 6.34 | 5.79 | 4.81 | 2.94 | 0.92 |
| NRG-2:1 | 32.26 | 25.84 | 31.79 | 10.11 | 4.84 | 3.88 | 4.77 | 1.52 |
| NRG-5:1 | 47.58 | 29.35 | 20.04 | 3.03 | 5.67 | 3.50 | 2.39 | 0.36 |
| NRG-5 | 37.51 | 41.38 | 18.95 | 2.16 | 5.64 | 6.22 | 2.85 | 0.32 |
| NRG-10 | 32.26 | 25.84 | 31.79 | 10.11 | 4.84 | 3.88 | 4.77 | 1.52 |
| NRG-20 | 32.32 | 19.32 | 46.06 | 2.30 | 3.43 | 2.05 | 4.89 | 0.24 |
| NRG-30 | 41.78 | 13.01 | 44.95 | 0.27 | 4.48 | 1.40 | 4.82 | 0.03 |

437  * $N_{py}$, $N_{pr}$, $N_g$, $N_o$, and $N_T$ represents pyridinic, pyrrolic, graphitic, oxidized and total N amount,

438  respectively.

439

440

441

442

443

444

445

446 **Table S4** Organic contents in P-T samples.

| Sample | Weight of precursor (g) | Weight of precursor after pyrolysis (g) | Weight of precursor after pyrolysis and acid washing (g) | Organic proportion In P-T (%) |
|---|---|---|---|---|
| P-340 | 10.0 | 4.8 | 1.1 | 23 |
| P-660 | 10.0 | 4.2 | 1.0 | 24 |

447

448

449

450

451

452

453

454

455

456

457

458

459

460

461

462

463

**References**

1.  Y. Xie, Y. Zhuo, S. Liu, Y. Lin, D. Zuo, X. Wu, C. Li and P. K. Wong, *Sol. RRL*, 2020, **4**, 1900440.

2.  A. Wang, Z. Zheng, H. Wang, Y. Chen, C. Luo, D. Liang, B. Hu, R. Qiu and K. Yan, *Appl. Catal. B: Environ.*, 2020, **277**, 119171.

3.  G. Kresse and J. Hafner, *Phys. Rev. B.* , 1994, **49**, 14251-14269.

4.  S. Grimme, J. Antony, S. Ehrlich and H. Krieg, *J. Chem. Phys.*, 2010, **132**, 154104.

5.  G. Kresse and D. Joubert, *Phy. Rev. B* 1999, **59**, 1758-1775.

6.  C. Zhang, L. Fu, N. Liu, M. Liu, Y. Wang and Z. Liu, *Adv. Mater.*, 2011, **23**, 1020-1024.

7.  G. Huang, J. Han, F. Zhang, Z. Wang, H. Kashani, K. Watanabe and M. Chen, *Adv. Mater.*, 2019, **31**, 1805334.

8.  L. Lin, J. Li, Q. Yuan, Q. Li, J. Zhang, L. Sun, D. Rui, Z. Chen, K. Jia, M. Wang, Y. Zhang, M. Rummeli, N. Kang, H. Q. Xu, F.mDing, H. Peng and Z. Liu, *Sci. Adv.*, 2021, **5**, 8337.

9.  L. Chen, J. Han, Y. Ito, T. Fujita, G. Huang, K. Hu, A. Hirata, K. Watanabe and M. Chen, *Angew. Chem. Int. Ed.*, 2018, **57**, 13302-13307.

10. Z. Sun, Z. Yan, J. Yao, E. Beitler, Y. Zhu and J. M. Tour, *Nature*, 2010, **468**, 549-552.

11. X. Fei, J. Neilson, Y. Li, V. Lopez, S. J. Garrett, L. Gan, H. J. Gao and L. Gao, *Nano Lett.*, 2017, **17**, 2887-2894.

12. Y. Wang, Y. Shao, D. W. Matson, J. Li and Y. Lin, *Acs. Nano*, 2010, **4**, 1790-1798.

13. U. Bangert, W. Pierce, D. M. Kepaptsoglou, Q. Ramasse, R. Zan, M. H. Gass, J. A. Van den Berg, C. B. Boothroyd, J. Amani and H. Hofsass, *Nano Lett*, 2013, **13**, 4902-

486    4907.

487  14.   L. S. Panchakarla, K. S. Subrahmanyam, S. K. Saha, A. Govindaraj, H. R.

488         Krishnamurthy, U. V. Waghmare and C. N. R. Rao, *Adv. Mater.*, 2009, **21**, 4726-4730.

489  15.   Y. Yuan, T. Wang, H. Chen, S. M. Mahurin, H. Luo, G. M. Veith, Z. Yang and S. Dai,

490         *Angew. Chem. Int. Ed.*, 2020, **59**, 21935-21939.

491  16.   X. Li, H. Wang, J. T. Robinson, H. Sanchez, G. Diankov and H. Dai, *J. Am. Chem. Soc.*,

492         2009, **131**, 15939-15944.

493  17.   J. Han, G. Huang, Z. Wang, Z. Lu, J. Du, H. Kashani and M. Chen, *Adv. Mater.*, 2018,

494         **30**, 1803588.

495  18.   J. Xu, M. Wang, N. P. Wickramaratne, M. Jaroniec, S. Dou and L. Dai, *Adv. Mater.*,

496         2015, **27**, 2042-2048.

497  19.   J. Sun, S. E. Lowe, L. Zhang, Y. Wang, K. Pang, Y. Wang, Y. Zhong, P. Liu, K. Zhao,

498         Z. Tang and H. Zhao, *Angew. Chem. Int. Ed.*, 2018, **57**, 16511-16515.

499  20.   Z. Wen, X. Wang, S. Mao, Z. Bo, H. Kim, S. Cui, G. Lu, X. Feng and J. Chen, *Adv.*

500         *Mater.*, 2012, **24**, 5610-5616.

501  21.   J. Liu, Y. Zhang, L. Zhang, F. Xie, A. Vasileff and S. Z. Qiao, *Adv. Mater.*, 2019, **31**,

502         1901261.

503  22.   X. Li, Z. Ao, J. Liu, H. Sun, A. I. Rykov and J. Wang, *ACS. Nano*, 2016, **10**, 11532-

504         11540.

505  23.   X. Li, X. Huang, S. Xi, S. Miao, J. Ding, W. Cai, S. Liu, X. Yang, H. Yang, J. Gao, J.

506         Wang, Y. Huang, T. Zhang and B. Liu, *J. Am. Chem. Soc.*, 2018, **140**, 12469-12475.

507  24.   G. Fang, T. Zhang, H. Cui, D. D. Dionysiou, C. Liu, J. Gao, Y. Wang and D. Zhou,

508     *Environ. Sci. Technol.*, 2020, **54**, 15489-15498.

509  25.    A. Wang, Y. Chen, Z. Zheng, H. Wang, X. Li, Z. Yang, R. Qiu and K. Yan, *Chem. Eng.*

510     *J.*, 2021, **411**, 128497.

511  26.    S. Xin, G. Liu, X. Ma, J. Gong, B. Ma, Q. Yan, Q. Chen, D. Ma, G. Zhang, M. Gao and

512     Y. Xin, *Appl. Catal. B: Environ.*, 2021, **280**, 119386.

513  27.    S. Ye, G. Zeng, X. Tan, H. Wu, J. Liang, B. Song, N. Tang, P. Zhang, Y. Yang, Q. Chen

514     and X. Li, *Appl. Catal. B: Environ.*, 2020, **269**, 118850.

515  28.    J. Zhou, F. Ma, H. Guo and D. Su, *Appl. Catal. B: Environ.*, 2020, **269**, 118784.

516  29.    F. Chen, L. L. Liu, J. J. Chen, W. W. Li, Y. P. Chen, Y. J. Zhang, J. H. Wu, S. C. Mei,

517     Q. Yang and H. Q. Yu, *Water Res.*, 2021, **191**, 116799.

518  30.    S. Guo, H. Wang, W. Yang, H. Fida, L. You and K. Zhou, *Appl. Catal. B: Environ.*,

519     2020, **262**, 118250.

520  31.    X. Hou, X. Huang, F. Jia, Z. Ai, J. Zhao and L. Zhang, *Environ. Sci. Technol.*, 2017, **51**,

521     5118-5126.

522  32.    H. Wang, T. Chen, D. Chen, X. Zou, M. Li, F. Huang, F. Sun, C. Wang, D. Shu and H.

523     Liu, *Appl. Catal. B: Environ.*, 2020, **260**, 118203.

524  33.    D. Xing, Z. Cui, Y. Liu, Z. Wang, P. Wang, Z. Zheng, H. Cheng, Y. Dai and B. Huang,

525     *Appl. Catal. B: Environ.*, 2021, **290**, 120029.

526  34.    H. Wang, Y. Wu, M. Feng, W. Tu, T. Xiao, T. Xiong, H. M. Ang, X. Yuan and J. Chew,

527     *Water Res.*, 2018, **144**, 215-225.

528  35.    M. Li, P. Wang, Z. Ji, Z. Zhou, Y. Xia, Y. Li and S. Zhan, *Appl. Catal. B: Environ.*,

529     2021, **289**, 120020.

530  36.    L. Zhou, S. Dai, S. Xu, Y. She, Y. Li, S. Leveneur and Y. Qin, *Appl. Catal. B: Environ.*,

531        2021, **291**, 120019.

532  37.    P. Yang, C. Chen, D. Wang, H. Ma, Y. Du, D. Cai, X. Zhang and Z. Wu, *Appl. Catal. B:*

533        *Environ.*, 2021, **285**, 119877.

534  38.    B. Shao, Z. Liu, G. Zeng, Y. Liu, Q. Liang, Q. He, T. Wu, Y. Pan, J. Huang, Z. Peng, S.

535        Luo, C. Liang, X. Liu, S. Tong and J. Liang, *Appl. Catal. B: Environ.*, 2021, **286**,

536        119867.

537  39.    F. Chen, Q. Yang, X. Li, G. Zeng, D. Wang, C. Niu, J. Zhao, H. An, T. Xie and Y. Deng,

538        *Appl. Catal. B: Environ.*, 2017, **200**, 330-342.

539  40.    Q. Zhang, L. Jiang, J. Wang, Y. Zhu, Y. Pu and W. Dai, *Appl. Catal. B: Environ.*, 2020,

540        **277**, 119122.

541  41.    P. Jin, L. Wang, X. Ma, R. Lian, J. Huang, H. She, M. Zhang and Q. Wang, *Appl. Catal.*

542        *B: Environ.*, 2021, **284**, 119762.

543  42.    H. Li, S. Sun, H. Ji, W. Liu and Z. Shen, *Appl. Catal. B: Environ.*, 2020, **272**, 118966.

544